TÉCNICO LISBOA

Viscosity Electronic Measurement Estimation System based on the Impedance Frequency response of a Vibrating Wire Sensor

Pedro Santos Rocha Madeira Marques

Thesis to obtain the Master of Science Degree in

Electronics Engineering

Supervisor: Prof. Pedro Miguel Pinto Ramos

Examination Committee

Chairperson:	Prof. Rui Manuel Rodrigues Rocha
Supervisor:	Prof. Pedro Miguel Pinto Ramos
Member of the Committee:	Prof. António Joaquim dos Santos Romão Serralheiro

May 2016

Acknowledgements

Firstly, I would like to thank my supervisor Professor Pedro Ramos for suggesting and giving me the opportunity to work on this subject, as well as for his advice and critical observations throughout this project.

To my family, for their support and encouragement during my struggles, who despite my absences was always there, not just to give their support but also to share my happy moments and experiences, during my academic years.

I would also like to thank all my colleagues and friends, who accompany me during this time of fun and hard work. A special thank you to both Fábio Barroso and Ruben Afonso, who put up with me during this entire course and whose help and friendship was and is of great importance.

A special thank you to Sr. João Pina dos Santos for all the advice and help given, not only during this project, but also in all the others I had to develop during this past few years.

Pedro Marques

Abstract

Nowadays, viscosity measurements play an important role in several areas, such as Industrial, Scientific and Technological, and have utility in various applications. In the Industrial area, viscosity measurements can be applied in several areas, such as the food, pharmaceutical, automobile, chemical and petroleum industries. Viscosity measurement brings benefits since monitoring it allows cost reduction as well as increased product quality and client satisfaction.

The viscosity measurement method used in order to develop this work, is based on a vibrating wire sensor. Its model and operating principle takes into account a set of equations and represents a system capable of making accurate impedance measurements, without which it would not be possible to obtain viscosity values.

This work aimed to develop a system capable of performing sensor's impedance measurements, characterization of that impedance for a particular range of frequency values, resonance frequency and half-height width estimations. Impedance measurements are of great importance because with them is possible to determine viscosity.

The system developed is based on a DSP as the central processing unit and a signal generator whose reference clock frequency is defined by the DSP. This characteristic allows a synchronism between signal generation and signal acquisition, made by two ADCs, whose reference clock frequency is also given by the DSP. The signal generation, studied, is responsible for the measurement circuit excitation, allowing the signal acquisition by the ADCs. Taking into account the theoretical equations, as well as the impedance values measured, it is possible to determine viscosity by studying the sensor's response to frequency variations.

This new approach, regarding the synchronism between signal generation and acquisition, allows a reduction of the digital processing required to determine viscosity making its process quicker. It was also implemented the USB interface in order to allow the connection to a personal computer so that the user could control the system, as well as view measured results.

Keywords: Viscosity, Vibrating Wire Sensor, DSP, Digital Processing, Synchronism.

Resumo

Nos dias que correm as medidas do valor de viscosidade desempenham um papel muito importante em diversas áreas e têm utilidades em variadas aplicações. São exemplos dessas, as áreas tecnológicas, científica e industrial. No caso da indústria, são vastos os sectores nos quais a medida de viscosidade pode ser aplicada, sendo exemplo disso, os sectores alimentar, farmacêutico, automóvel, químico e petrolífero, onde a medição da viscosidade traz benefícios, uma vez que o seu controlo possibilita a redução de custos, bem como o aumento da qualidade de produto e por conseguinte satisfação do cliente.

O método de medida da viscosidade utilizado no desenvolvimento deste trabalho, recorre à utilização de um sensor de fio vibrante. O princípio de funcionamento deste tem em conta um conjunto de equações e representa um sistema capaz de efectuar medidas de impedâncias exactas, sem as quais não seria possível obter valores de viscosidade.

Este trabalho teve como objectivo desenvolver um sistema capaz de efectuar medidas de impedância do sensor, caracterizar essa impedância para uma determinada gama de valores de frequência e estimar a frequência de ressonância e a largura de meia altura, sendo que estes parâmetros são de grande importância, pois sem estes não seria possível fazer o cálculo da viscosidade.

O sistema desenvolvido baseou-se num DSP como unidade de processamento e num gerador de sinais, cuja frequência de referência de relógio é fornecida pelo DSP, o que permite que exista um sincronismo entre geração e aquisição de sinais, sendo que esta é feita por dois ADCs, cuja frequência de referência de relógio é também fornecida pelo DSP. O gerador de sinais é responsável por excitar o circuito de medida, permitindo aos ADCs fazer aquisição dos sinais necessários para a determinação da impedância do sensor. Assim, e tendo em conta as equações teóricas que modelam o sensor, é possível estudar o comportamento do mesmo face a variações da frequência, o que possibilita determinar a frequência de ressonância, a largura de meia altura e por fim a viscosidade.

Esta nova abordagem, no que respeita ao sincronismo entre aquisição e geração, possibilita uma redução do processamento digital necessário ao cálculo da viscosidade, tornando assim o processo de medida mais rápido. Foi ainda implementada interface USB, por forma a possibilitar a ligação a um computador pessoal, permitindo a visualização de dados, bem como controlo do sistema.

Palavras – Chave: Viscosidade, Sensor de Fio Vibrante, DSP, Processamento Digital, Sincronismo.

Table of Contents

List of Figures

List of Tables

List of Acronyms

AC	Alternate Current
ADC	Analog to Digital Converter
AMPOP	Operational Amplifier
DAC	Digital to Analog Converter
DC	Direct Current
DDS	Direct Digital Synthesizer
DSP	Digital Signal Processor
dsPIC	Digital Signal Peripheral Interface Controller
FFT	Fast Fourier Transform
FG	Function Generator
GPIB	General Purpose Interface Bus
IA	Instrumentation Amplifier
I^2C	Inter-Integrated Circuit
I/O	Input/Output
IpDFT	Interpolated Discrete Fourier Transform
LUT	Look-Up-Table
NIST	National Institute of Standards and Technology
PGA	Programmable Gain Amplifier
PIC	Peripheral Interface Controller
PC	Personal Computer
PWM	Pulse-Width Modulation
RAM	Random-Access Memory
RMS	Root Mean Square
SDRAM	Synchronous Dynamic Random-Access Memory
SI	International System
SPI	Serial Peripheral Interface
SNR	Signal-to-Noise Ratio
UART	Universal Asynchronous Receiver/Transmitter
USB	Universal Serial Bus

1 Introduction

This chapter is divided into three parts. The first one is a small introduction of the work developed, as well as the applications involving it and its main characteristics. The second part approaches the goals that were intended to be accomplished and the challenges that needed to be surpassed. On the third and final part of this chapter, a brief summary of this report's organization, is made.

1.1 Purpose and Motivation

When it comes to predicting how a liquid material will behave in the real world, viscosity is an important measure that needs to be done and therefore gathering information in regards to this property is very relevant. It is important in several areas, such as food and petroleum industries, cosmetics, and pharmaceuticals.

In the food industry, viscosity plays a big role since measuring it will maximize production efficiency and cost effectiveness. For example, it affects the time a fluid takes to be dispensed into packaging, when talking about production efficiency and it is also a characteristic of food's texture which is important when talking about customer satisfaction. In cosmetics, viscosity should be considered when designing the feel and flow of cosmetic products for the skin. As for petroleum industry it is important to determine its economic viability due to the fact that the viscosity of a crude oil affects its ability to pump it out of the ground. It is also important in the automotive area to ensure the quality of motor and fuel oils. Taking into account the different uses for viscosity measurements, it is important to have measurement methods with the ability to conduct them in a fast, precise and reliable way [1].

From the end-user point of view, the only viscosity referent point accepted so far is the viscosity of pure water at 293.15 K at atmospheric pressure. The existence of just a single reference point is quite unsatisfactory, as the viscosity of fluids can vary by a large factor of 10^{14} [2]. The fact that water is the only reference point accepted is mostly due to the fact that, up to now, it has not been possible to establish a primary method of measurement for the different ranges of viscosity. Because of that, over time there have been made efforts aiming to the development of new viscosity measurement methods.

Among the different methods for measuring viscosity, the method based on the vibrating wire has proven itself quite versatile, since it presents greater ease in construction, can be operated remotely and can be used in a wide range of temperatures and pressures without the need for calibration on the ranges upon which the measures are made [3]. These advantages are mostly due to the fact that the vibrating wire sensor is entirely composed of solids, which allows accurate measures when submitted to temperature and pressure changes, on the sensor's components. It is also supported by a rigorous theory, the vibrating wire technique, which does not require extensive calibration procedures [4].

One of the parameters that the vibrating wire sensor requires to measure viscosity is the sensor's impedance response for a certain range of frequencies around the resonance frequency. The impedance value is determined based on the voltage at the sensor's terminals and on the current applied

to the circuit. Therefore, the method chosen and studied takes advantage of a reference impedance, whose value is well known, allowing the measurement of the sensor's impedance, by applying time and frequency domain algorithms on the processing unit.

1.2 Goals and Challenges

The main objective of this thesis was to develop, implement and characterize an electric system for liquid's viscosity measurements, thought the use of a vibrating wire sensor. In order to accomplish this work, some intermediate objectives needed to be completed:

- Dimensioning of the analog circuit interface between the generator and the vibrating wire sensor;
- Define the range of signals for the generator that needs to be developed;
- Define the range of the output signals for the vibrating wire sensor;
- System testing by using an acquisition board and commercial function generator with the sensor inserted inside liquids with different viscosities;
- Determine the linear operating zones;
- Development of optimizing algorithms that allow the estimation of viscosity by minimizing the number of measured frequencies;
- Development of analog conditioning circuits for input and generated signals;
- Selection and test of the processing unit;
- Definition and implementation of communication protocols between the system developed and the exterior control unit (computer);
- Implementation and prototyping of the electric system;
- Implementation of estimation algorithms on the processing unit;
- Characterizing measurements for the device;
- Measurement of different viscosities;
- System calibration;
- Presentation of the results.

1.3 Document Organization

Chapter two contains an overview about viscosity and impedance concepts, as well as reference liquids used in order to acquire valid viscosity values. Some viscosity and impedance measurement methods and its applications are presented. It is also described the vibrating wire sensor that was used, in order to determine viscosity.

In chapter three the architecture, system structure and methodology of the project are presented, as well as the description of the fundamental parts that where developed, as well as the algorithms studied.

Chapter four revolves around the system software developed and approaches the communication between the different modules of the system, as well as the personal computer and its user.

In chapter five, some experimental results are showed and in chapter six some conclusions concerning the current state of the project, design constraints and objectives that were not concluded, are presented.

Lastly in chapter seven, is presented the future work suggested, in order to improve the work that was developed.

2 State of the Art

On this chapter is the studied the main concepts needed to the development of this project. It revolves around viscosity concept, viscosity measurement methods as well as liquid materials used for reference when making viscosity measures. Besides that, because of its importance, impedance concept and impedance measurements methods have also been studied, and therefore are addressed in this chapter.

2.1 Viscosity Concept

Viscosity is as a measure upon which a fluid's tendency to dissipate energy is perturbed from equilibrium by a force field, leading the fluid to be distorted at a given rate. Viscosity depends of the thermodynamic of the fluid state and in the case of a pure fluid, it is usually specified by a pair of variables, temperature and pressure or temperature and density. In the case of mixtures composition, dependences must also be measured [2].

There are actually two quantities called viscosity, the dynamic or absolute viscosity and the kinematic viscosity. Dynamic viscosity can be demonstrated by the use of two parallel layers with a fluid between them, as shown in Figure 2.1. While maintaining the lower layer stationary, separated from the upper layer by a distance y_0, and by applying an external force to the upper layer giving it a constant velocity v_0, the fluid near it will also move.

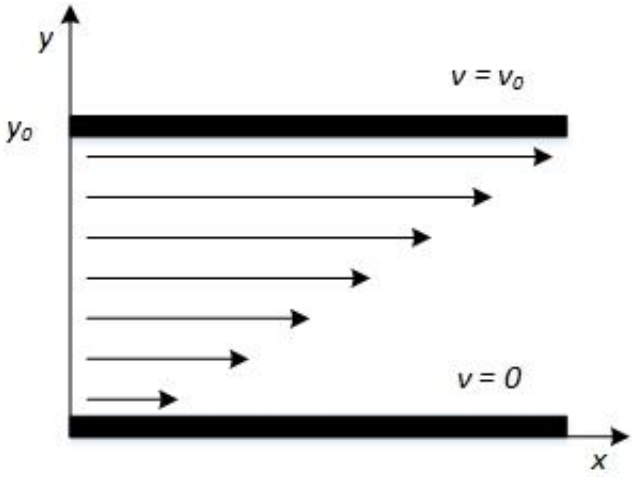

Figure 2.1 - Velocity Gradient between two Plates. Adapted from [11].

This effect can be described by

$$\frac{F}{A} = \eta \frac{\Delta V}{\Delta y} = \eta \frac{v_0 - 0}{y_0 - 0} = \eta \frac{v_0}{y_0}, \tag{2.1}$$

where the force applied in order to move the upper layer is represented by F, per unite area A, η represents the viscosity of the fluid between the two layers, $\left(\frac{F}{A}\right)$ the shearing stress and $\left(\frac{\Delta V}{\Delta y}\right)$ the velocity

gradient. Therefore, viscosity is the ratio between the shearing stress to the velocity gradient, and its SI unit is Pascal second [Pa.s].

As for the kinematic viscosity ν, it is the ratio of the absolute viscosity of a fluid to its density ρ,

$$\nu = \frac{\eta}{\rho}, \tag{2.2}$$

It can be used to measure the resistive flow of fluids under the influence of gravity. It is frequently measured by using capillary viscometers, which will be explained in section 2.2.1. The SI unit for kinematic viscosity is square meter per second [m^2/s].

When it comes to factors affecting viscosity's behaviour, some must be taken into account. From common knowledge based on everyday experience, viscosity varies with temperature. For instance, fluids such as honey, when heated, will flow more easily. In liquids, as temperature increases the average speed of the molecules will rise and the amount of time they spend with their nearest neighbours will decrease whereas some gases do not behave the same way, instead of increasing their easiness to flow they will get thicker when heated.

2.2 Viscosity Measurement Methods

There are several methods to measure fluid's viscosity. They can be divided into two categories, quasi-primary and secondary methods. There are no primary methods since the ones that were developed so far, to achieve high accuracy, need to involve instrumental parameters obtained through calibration, in other words, quasi-primary methods are the ones that make use of physically working equations that relate viscosity to parameters already measured experimentally. Oscillating Body and Vibrating Wire Viscometers are an example of quasi-primary methods. As for the secondary methods, they are the ones upon which there is no detailed knowledge of the fluid's mechanics to be applied in order to correct measures done experimentally. Capillary and Falling Body Viscometers belong in this category [2].

2.2.1 Capillary Viscometers

Capillary Viscometers or U-tube Viscometers, presented in Figure 2.2, are the ones used more extensively when it comes to measuring viscosity, especially in liquids.

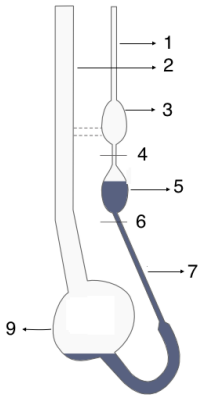

Figure 2.2 - Capillary Viscometer Example. Adapted from [6].
1 - Tube with capillary; 2 - Venting Tube; 3 - Pre-Run Sphere; 4 - Upper Timing Mark; 5 - Measuring Sphere; 6 - Lower Timing Mark; 7 - Capillary; 8 - Reservoir.

They consist in a U-shaped glass tube, which is held vertically in a controlled temperature bath. This type of viscometer is based on the dynamics of Hagen-Poiseuille Equation. For compressible fluids, it relates the volumetric flow rate, Q, of the tube carrying the fluid, with its radius, length, pressure difference and viscosity coefficient,

$$Q = \frac{\pi R^4 (P_i - P_o)}{8\eta L}, \tag{2.3}$$

where R and L are the radius and length of the tube, P_i and P_o are the pressure between the start and the end of the tube and η is the fluid's viscosity [5][6].

However, the use of this type of viscometer requires some calibration due to the extreme difficulty in measuring viscosity and involves some experimental difficulties, such as the requirement of special thermostatic baths that need a constant temperature control for large depths.

2.2.2 Falling Body Viscometers

Falling body viscometers make use of the time of a free falling body of revolution[1], normally a sphere or a cylinder, under the influence of gravity, through a fluid whose viscosity needs to be measured. This method is based on Stokes' law [3][7], which refers to the friction force that spherical objects suffer while moving within a viscous fluid,

$$F_d = 6\pi\eta R v, \tag{2.4}$$

[1] Surface created by rotating a curve around an axis of rotation.

where F_d is the frictional force, R the radius of the spherical object, v the particle's velocity and η the dynamic viscosity. In the event of a vertical drop of the object, it is possible to calculate the terminal velocity v_S, by relating the frictional force with gravity force

$$v_S = \frac{2R^2 g(\rho_p - \rho_f)}{9\eta}, \tag{2.5}$$

where ρ_p and ρ_f are the particle and fluid mass density, respectively [8].

Even though this type of viscometers have multiple advantages when it comes to operations with high pressure or as relative instruments for industrial applications, they need calibrations by using standardized liquids, and present an uncertainty of around $\pm$3% [3]. Also, they have restrictions related to the impossibility of ensuring that the body and the tube are completely cylindrical and that the first one falls according to the axis of the second without rotational movement. Also, to apply this method, the use of a very low Reynolds number[1] is required, making it dependable on storage and image processing [9][10].

2.2.3 Oscillating Body Viscometers

Just like the previous method, oscillation body viscometers, represented in Figure 2.3, can be used with different shaped bodies, such as disks, cups, cylinders and spheres. Disks are currently the most accurate for measurements in both gas and liquid phases.

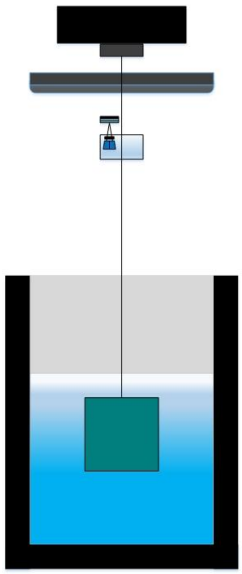

Figure 2.3 - Oscillating Body Viscometer. Adapted from [9].

These types of viscometers require a perfect parallel alignment of the fixed plates and the disk, as well as their flatness, to achieve acceptable measurements. They work by applying a force on the oscillating body while the fluid involving it exercises a contrary force to its surface, increasing the oscillating period and reducing the amplitude of the angular movement. This effect, along with the

[1] Dimensionless quantity used in fluid mechanics to help predict similar flow patterns in different fluid situations.

theoretical equations, allow an assessment of the viscosity. The most accurate measurements in the fluid state obtained with this type of device, are in the free-decay mode of operation, and uncertainties better than 1 % can be achieved [2].

2.2.4 Surface Light Scattering Spectroscopy

This technique analyses the dynamics that surface fluctuations present at the phase boundary of the fluid system under investigation, at a given wave vector. In contrast to conventional systems already mentioned, this one allows the determination of viscosity and interfacial tension in macroscopic thermodynamic equilibrium.

It is an absolute method since it as no need for calibration procedure using a fluid of known viscosity. However, it cannot yet be considered a primary method of measurement because it is still necessary, in addition to the density of the liquid phase, to have information about the density and viscosity of the gaseous phase under saturation conditions [2][11].

2.2.5 Torsionally Oscillating Quartz Crystal

This viscometer is based on the excitation of a quartz crystal that is cut along its optical axis and presents a radiofrequency signal at its surface that produces microscopic torsional vibrating movements [2].

When the crystal is immersed in a viscous medium, its vibrations will induce a viscous wave that will be rapidly attenuated by the medium. Since the viscous drag exerted by the fluid on the surface of the crystal changes its resistance and resonance frequency, from those in vacuum, it is possible to know the product of viscosity and density of the fluid, by measuring the conductance and capacitance properties of the crystal.

One of the advantages over the other type of viscometers is the fact that it has no moving parts and therefore its application has a wider range of temperatures and pressures. However, the requirement of independent viscosity data to enable the calculation of the quality factor of the oscillator in vacuum imposes a restriction to its use.

2.2.6 Vibrating Wire Viscometers

Vibrating wire viscometers are in a way related with oscillating body viscometers, but instead of torsional oscillatory movements these use transversal movements. This type of viscometers involve the distortion, by an external applied field, of a solid body, normally a wire as it can be seen in Figure 2.4, immersed in the fluid. When working in a forced mode of operation, the characteristics of the resonance curve for the transverse oscillations of the wire are correspondingly determined by the viscosity and density of the fluid. In other words, the surrounding fluid will exert an effect on the period and amplitude of oscillation allowing viscosity measurements [2].

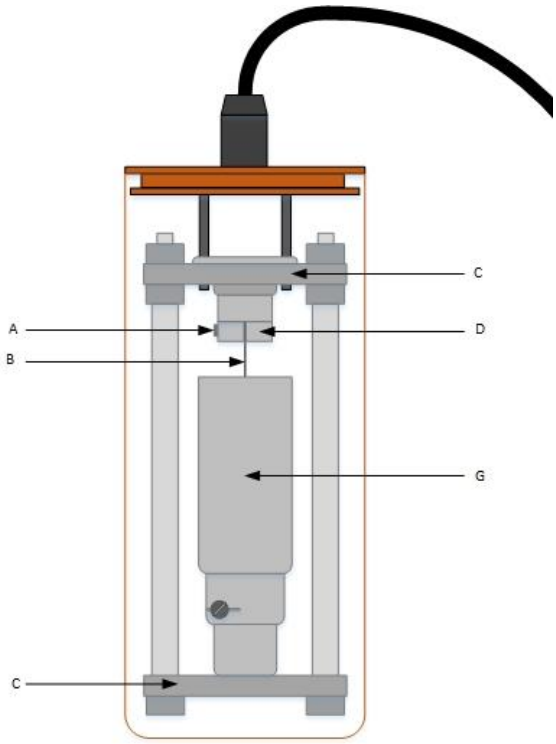

Figure 2.4 - Vibrating Wire Sensor.
A - Wires Tension adjustment Screw; B - Vibrating Wire; C - Fixing Plates; D - Magnets; G - Vase.

As shown in Figure 2.4, the vibrating wire sensor is placed inside a cell composed by two parallel magnetic plates on each end, with a wire fixed between them, submerged in the fluid to be studied [3][12]. Its principle of measurement is based on Lorentz Force[1], which is generated by applying an electric current inside a magnetic field, first to create the oscillatory movement and then to detect the vibration, since an electric voltage is induced.

To perform measurements, an alternate current must be forced in the wire and a sweep in frequency around the resonance frequency must be made. Since the wire is subjected to a magnetic field, created by the parallel magnetic plates, the forced current will cause transversal oscillations on the wire allowing the current frequency to vary and therefore enabling to determine the sensor's response in frequency. By analysing the sensor's impedance for an interval where the resonance frequency is contained, it is possible to determine the resonance characteristics of the transversal oscillations of the wire [9]. Therefore, to use these devices to determine the viscosity, a set of equations that characterize and translate the principle upon which they work, as well as the frequency response of the sensor, must be taken into account. A theoretical model of the vibrating wire was developed in [13], which is based on its oscillatory characteristics when surrounded by a fluid.

Vibrating wire instruments can be operated in a free decay mode and in a forced mode. In the first one, the wire is put in a state of oscillation and then left freely until it stops. As for the second one, which is the one used in this project, due to the difficulties of operating in the free decay mode, is described as a sweep in frequency around the resonance frequency, whose solution is given by

[1] Combination of electric and magnetic force on a point charge due to electromagnetic fields.

$$\frac{\partial}{\partial\widetilde{\omega}}\left\{\widetilde{\omega}^2(\beta'+2\Delta_0)^2+\left[\widetilde{\omega}(1+\beta)-\frac{\widetilde{\omega}_0^2}{\widetilde{\omega}}\right]^2\right\}=0, \tag{2.6}$$

with the half-height width,

$$\Delta\omega = \omega_+ - \omega_-, \tag{2.7}$$

of the resonance curve, related with the cell parameters through

$$\frac{\widetilde{\omega}_\pm(\beta'+2\Delta_0)}{{\widetilde{\omega}_\pm}^2(\beta'+2\Delta_0)^2+\left[\widetilde{\omega}_\pm(1+\beta)-\frac{\widetilde{\omega}_0^2}{\widetilde{\omega}_\pm}\right]^2} = \frac{1}{2}\frac{\widetilde{\omega}_r(\beta'+2\Delta_0)}{{\widetilde{\omega}_r}^2(\beta'+2\Delta_0)^2+\left[\widetilde{\omega}_r(1+\beta)-\frac{\widetilde{\omega}_0^2}{\widetilde{\omega}_r}\right]^2}, \tag{2.8}$$

where the average power is equal to half of its maximum value, which occurs on the resonance frequency [4].

In (2.6) and (2.8), the symbol (~), above the variables, corresponds to dimensionless quantities and therefore $\widetilde{\omega}_0$ represents the dimensionless natural frequency of oscillation of the wire, $\widetilde{\omega}_\pm$ the dimensionless half-height width and $\widetilde{\omega}_r$ the dimensionless resonance frequency. The relation between dimensionless quantities and angular frequency ω is

$$\widetilde{\omega} = \omega\sqrt{\frac{4\rho_s L^4}{ER^2}}, \tag{2.9}$$

where ρ_s, R and L are the density, radius and half-length of the wire, respectively. Variable E represents the Young's modulus[1] of the wire's material, ω_0 the natural frequency and Δ_0 the internal damping of the wire [13].

The oscillating characteristics of the vibrating-wire sensor depend of the fluid's density, ρ, and the fluid's viscosity, η, thought the functions β and β' which represent the additional mass and the viscous friction respectively. Therefore,

$$\beta = \left(\frac{\rho}{\rho_s}\right)k \tag{2.10}$$

and

$$\beta' = \left(\frac{\rho}{\rho_s}\right)k', \tag{2.11}$$

where the parameters k and k' are defined based on the treatment of the fluid's mechanics as

[1] Measure of the stiffness of an elastic material.

$$k = -1 + 2I(A), \tag{2.12}$$

$$k' = 2R(A). \tag{2.13}$$

In (2.12) and (2.13), the variable A is represented by

$$A = j\left[1 + \frac{2K_1\left(\sqrt{j\Omega}\right)}{\sqrt{j\Omega}K_0\left(\sqrt{j\Omega}\right)}\right]. \tag{2.14}$$

As for K_0 and K_1, they are two modified Bessel functions[1] with complex arguments and Ω a dimensionless frequency that is related with the Reynolds number for the fluid's movement around the wire and is given by

$$\Omega = \frac{\rho\omega R^2}{\eta}, \tag{2.15}$$

where R represents the radius of the wire, ρ and η the fluid's density and viscosity, respectively.

Using (2.6) to (2.15), it is possible to determine a fluid's viscosity, based on the resonance curve characteristics of the wire when submerged inside the fluid. To achieve that, it is required to know the radius of the wire and the fluid's density [3].

In the present work, to be able to determine the viscosity, it is required to know the sensor's response to frequency and to do that there is the need to connect the sensor's resonance curve with the expressions that model the electric circuit of the sensor, shown in Figure 2.5.

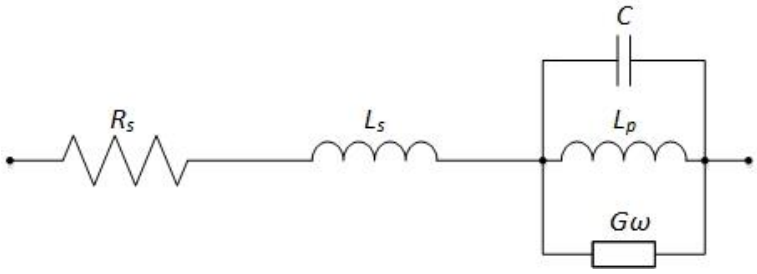

Figure 2.5 - Vibrating Sensor Electrical Model. Adapted from [4].

For that to be possible, an alternate current must be applied to sensor. This will cause oscillations on the wire, which are perpendicular to the direction of the magnetic field and imposed by the magnetic plates. According to Figure 2.5, the electric model of the sensor consists on a capacitance C, in parallel with an inductance L_p, and a conductance $\mathrm{G}\omega$, frequency dependent. The resistance R_s in series with the inductance L_s, model the resistance and inductance of the wire [3][4][12]. Therefore, the vibrating wire response can be interpreted as a complex impedance

[1] Canonical solutions of Bessel's differential equation for an arbitrary complex number.

$$\bar{Z} = R_s + j\omega L_s + \frac{1}{G\omega + j\omega C + \frac{1}{j\omega L_p}} \tag{2.16}$$

and by determining the module of $\bar{Z}$, it is possible to describe the resonance curve by

$$|\bar{Z}| = \sqrt{\frac{\left(1 + R_s G\omega - \omega L_s\left(\omega C - \frac{1}{\omega L_p}\right)\right)^2 + \left(R_s\left(\omega C - \frac{1}{\omega L_p}\right) + \omega^2 L_s G\right)^2}{G^2\omega^2 + \left(\omega C - \frac{1}{\omega L_p}\right)^2}}. \tag{2.17}$$

When the resonance curve, obtained experimentally is adjusted, it is possible to determine the parameters C, L_s, L_p, G and R_s, which are directly related with the hydromechanics' model equations. The resonance frequency, ω, and the half-height width of the resonance curve, (2.7), are obtained from the parallel elements of the electric circuit, which will result on a simplification of (2.17), written only in terms of the parameters G, ω, L_p and C [9]. Having said that

$$|\bar{Z}| = \frac{1}{\sqrt{G^2\omega^2 + \left(\omega C - \frac{1}{\omega L_p}\right)^2}}, \tag{2.18}$$

whereas the impedance value for the resonance frequency is

$$Z_{máx} = \frac{1}{2}\frac{\sqrt{2}}{\sqrt{\frac{C^2 + \sqrt{G^2 + C^2} \times C + G^2}{L_p\sqrt{G^2 + C^2}}}}. \tag{2.19}$$

As for the resonance frequency, it is

$$\omega_0 = \frac{1}{\sqrt{L_p\sqrt{G^2 + C^2}}}. \tag{2.20}$$

and the half-height width is

$$\Delta\omega = \frac{1}{L_p\sqrt{G^2 + C^2}}\left[\sqrt{A + B} - \sqrt{A - B}\right], \tag{2.21}$$

with

$$A = -L_p C + 2L_p\sqrt{G^2 + C^2} \tag{2.22}$$

and

$$B = \sqrt{-{L_p}^2\left(4C\sqrt{G^2+C^2}-3G^2-4C^2\right)}. \quad (2.23)$$

To summarize, by applying (2.20) and (2.21) the resonant frequency and half-height width of the vibrating wire sensor can be determined and by replacing those values in (2.6) and (2.8) and by knowing the sensor cell parameters, making it possible to determine the viscosity.

2.3 Reference Liquids

Among others, viscosity is a propriety of materials that presents a huge amount of importance for numerous scientific and technologic applications. However, it is one of the properties that have less reference values despite the measurement, correlation and interpolation studies that exist for it.

The only reference value of viscosity is the water at 293.15 K and at atmospheric pressure. Due to the fact that viscosity value can vary so much ranging from lower values, usually on gaseous fluids, to higher values, in metals and fused glass, the isolated value of water is insufficient for the technologic and industrial needs [3].

Water is the only substance chosen as primary reference material for measuring viscosity since it fulfils the necessary requisites in terms of availability, security and purity. Its current viscosity value accepted is based essentially on a set of measurements made on the National Institute of Standards and Technology (NIST), during a period of twenty years. There, on the year of 1952, Swindells, Coe and Godfrey referenced the viscosity value of water as (1.0019 $\pm$ 0.0003) mPa.s at 293.15 K. Since then, the reference value of water suffered some changes and the last value accepted was 1.0005 mPa.s $\pm$ 0.05 %, with a confidence level of 68 %, at 293.15 K [3].

Besides water, there are other materials that may yet be used as reference materials for viscosity, since they also fulfil the required requisites for that. Some of them are already used as reference materials on other properties, such as thermic conductivity and calorific capacity. For example, toluene is one of the substances that may be considered a reference material for viscosity, presenting itself on the liquid state in a wide range of temperatures and with a high purity. Besides toluene, other compounds like n-nonane, n-decane and n-undecane are being considered to become reference materials since they possess viscosity values close to the water, under ambient temperature and atmospheric pressure, with a wide range of temperatures in the liquid state, low water solubility, low vapour pressure and absence of response to most of the materials [3].

2.4 Impedance Concept

To characterize electronic circuits, depending on the application, there are several measurements that have to be made. Impedance is one of those important measurements that can be used to describe electronic circuits as well as components and materials used to make them. Also, when it comes to the characterization of transducers and sensors, measuring the impedance is quite important since it is

proportional to the variation of some physical phenomena like temperature, displacement or force and therefore can be used to translate non electrical information into the electrical domain.

Impedance, which is generally represented by $\bar{Z}$, is defined as the total resistance a device or circuit offers to the flow of an alternate current, at a given frequency [14]. Unlike resistances that only possess magnitude, impedance possesses both magnitude and phase and therefore it is represented as a complex quantity, as shown in Figure 2.6, where its graphical representation on a vector plane can be observed. Taking that into account, an impedance vector consists of a real part designated as a resistive component R and an imaginary part designated as a reactive component X.

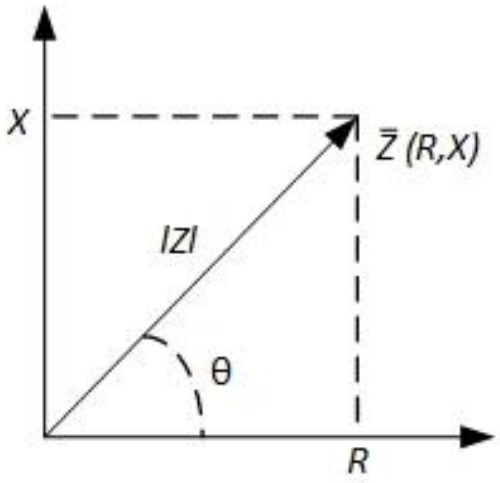

Figure 2.6 - Impedance Graphical Representation. Adapted from [14].

The unit used for impedance is ohms (Ω) and can be expressed in two forms. The rectangular form,

$$\bar{Z} = R + jX, \tag{2.24}$$

which, consists of two components, resistive and reactive, and the polar form which consists on a magnitude and a phase angle,

$$\bar{Z} = |Z|\, e^{jarg(\bar{Z})}, \tag{2.25}$$

where the argument $arg(\bar{Z})$, commonly given the symbol θ, gives the phase difference between voltage and current. The mathematical relationships between R, X, $|\bar{Z}|$ and θ can be described by

$$R = |\bar{Z}|\, cos\, \theta \tag{2.26}$$

$$X = |\bar{Z}|\ sin\, \theta \tag{2.27}$$

$$|\bar{Z}| = \sqrt{R + X} \tag{2.28}$$

$$\theta = tan^{-1}\left(\frac{X}{R}\right) \tag{2.29}$$

It is important to state that the reactive part of impedance can take two forms, inductive (X_L) and capacitive (X_C), as shown in Figure 2.7.

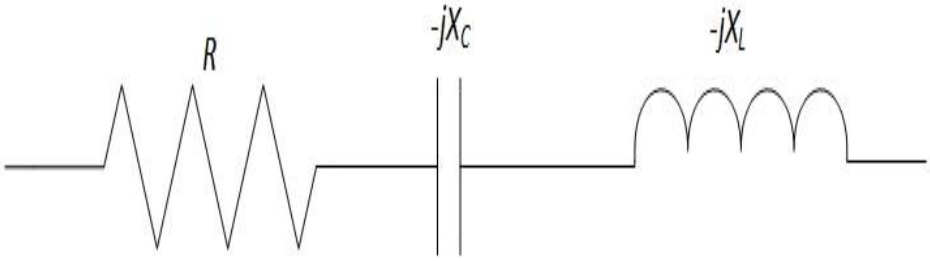

Figure 2.7 - Inductive and Capacitive Reactance. Adapted from [14].

The inductive reactance X_L is proportional to the signal frequency, whereas the capacitive reactance X_C is inversely proportional to the signal frequency.

2.5 Impedance Measurement Methods

To measure impedance, several methods can be applied and each and every one of them has its advantages and disadvantages. To select the best one, there are some conditions that must be taken into account, such as range of operating frequencies, accuracy and ease of operation.

2.5.1 Bridge Method

The bridge method, whose setup is presented in Figure 2.8, consists on measuring the unknown impedance $\overline{Z_X}$ by solving the relationship with the other bridge elements when $D = 0$,

$$\overline{Z_X} = \frac{\overline{Z_1}}{\overline{Z_2}}\overline{Z_3}. \tag{2.30}$$

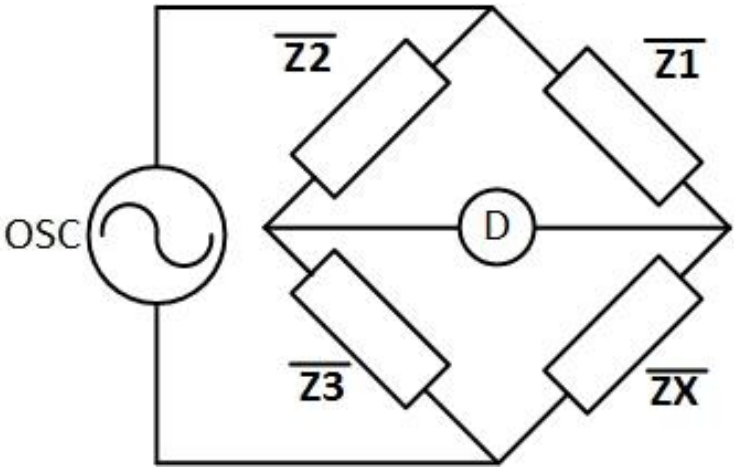

Figure 2.8 - Bridge Setup. Adapted from [14].

To apply this method there can be no current passing through the detector (D). Regarding the bridge circuits, there are several types that can be employed by using various combinations of L, C and R components, which will diversify the number of applications. Even though this method requires to be

manually balanced, it is low cost and has a wide frequency coverage ranging from DC to 300 MHz, through the use of different types of bridges [14].

2.5.2 Resonant Method

The setup for the resonant method, seen in Figure 2.9, is applied by tuning the capacitor C, to a resonant state.

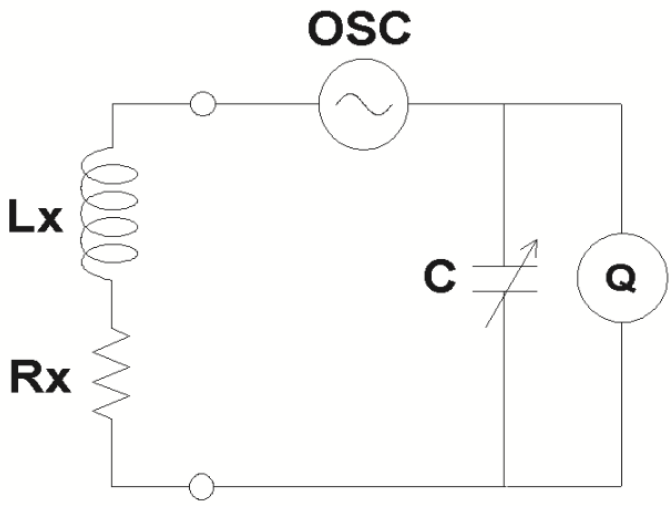

Figure 2.9 - Resonant Setup. Taken from [14].

When the resonance is obtained, the unknown impedances L_X and R_X values are obtained from C and Q values and from the test frequency. Q is the quality factor and can be measured directly by using a voltmeter placed across the tuning capacitor. Since the circuit presents very low losses, Q values measured can be as high as 300 [14].

2.5.3 I-V Method

The I-V, also known as volt-ampere method, is applied by measuring the unknown impedance $\overline{\mathrm{Z_X}}$ and is shown in Figure 2.10.

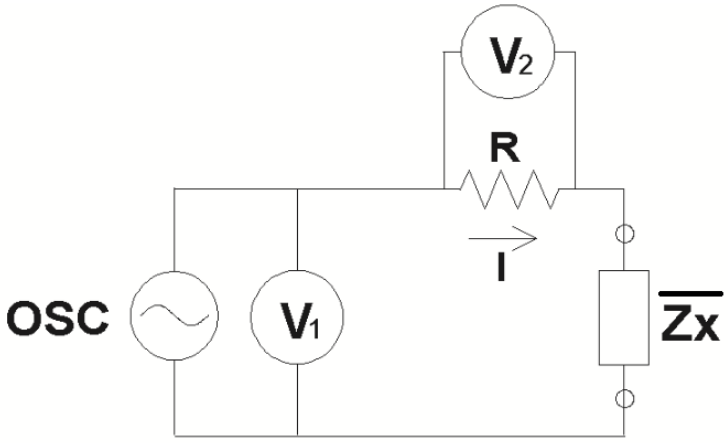

Figure 2.10 - Volt-Ampere Setup. Taken from [14].

To measure $\overline{Z_X}$ it is required to know the value of the voltage V_1 and the current I flowing through R. The current I is calculated by using the voltage measurement V_2 and by ensuring that the resistor R has a known low value. Therefore,

$$\overline{Z_X} = \frac{\overline{V_1}}{\overline{I}} = \frac{V_1}{V_2}R. \tag{2.31}$$

In practice, to prevent the effects caused by placing a low value resistor in the circuit, a low-loss transformer is used to replace it. However this solution brings downsides, since the use of a transformer limits the low end of the applicable frequency range [14].

2.5.4 RF I-V Method

The RF I-V method is similar to the I-V method, since it is based on the same principle, although its configuration is different. This method has two different configurations and uses an impedance matched measurement circuit (50 Ω) and a precision coaxial test port for operation at higher frequencies.

The two possible configurations, presented in Figure 2.11, differ in the fact that the one on the left is more suited for measuring low impedances up to 100 Ω, and the other is for measuring higher impedances ranging from 0.1 to 10 kΩ.

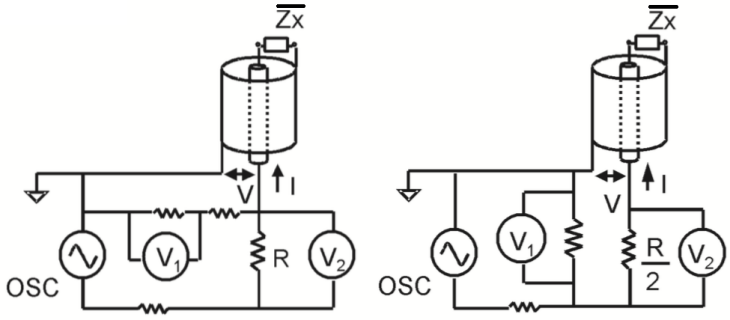

Figure 2.11 - RF I-V Setup for Low (left) and High (right) Impedances. Taken from [14].

Like in the I-V method, the principle used to measure the current that flows through the unknown impedance $\overline{Z_X}$ is based on the fact that the resistor R has a well known low value, allowing measuring the voltage across it. With that said, $\overline{Z_X}$ is calculated based on the measured voltage values V_1 and V_2 by

$$\overline{Z_X} = \frac{\bar{V}}{\bar{I}} = \frac{2R}{\frac{V_2}{V_1} - 1}, \tag{2.32}$$

for low impedances and

$$\overline{Z_X} = \frac{\bar{V}}{\bar{I}} = \frac{R}{2}\left(\frac{V_1}{V_2} - 1\right), \tag{2.33}$$

for higher impedances.

Just like before, a low loss transformer can be used in place of the resistor R, which will limit the low end of the frequency range [14].

2.5.5 Network Analysis

The network analysis method, which is used for higher frequency ranges, consists on measuring the reflection at the unknown impedance $\overline{Z_X}$, and is shown in Figure 2.12.

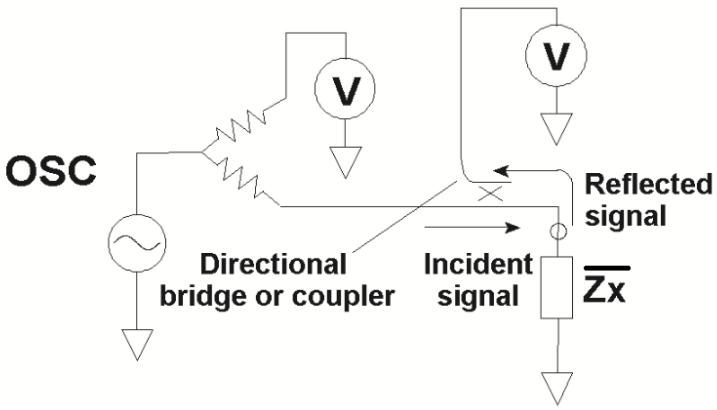

Figure 2.12 - Network Analysis Setup. Taken from [14].

The reflection coefficient is obtained by measuring the ratio between the incident and the reflected signals and in order to allow the detection of the reflected signal, a directional coupler or a bridge can be used. As for the supply and signal measuring, a network analyser is used [14].

2.5.6 Auto Balancing Bridge

The auto-balancing bridge method setup is showed in Figure 2.13.

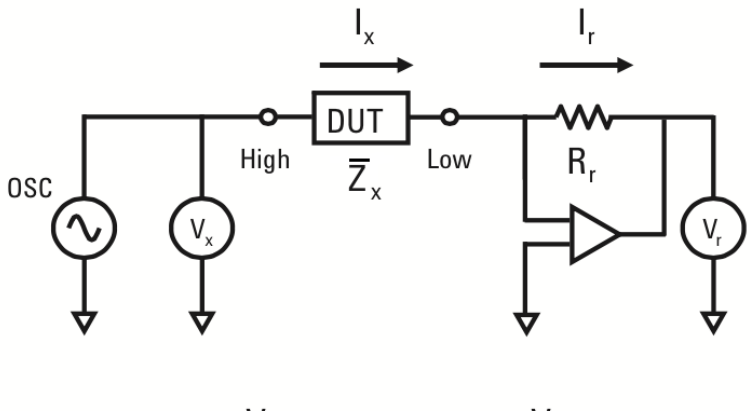

Figure 2.13 - Auto Balancing Bridge Setup. Taken from [14].

On this method, the current flowing through the unknown impedance $\overline{Z_X}$ also flows through the reference resistor R_r whose value is well known. Due to the balance between R_r and $\overline{Z_X}$, and thanks to the current passing through them, the potential at the "Low" point is maintained at zero Volts. Impedance $\overline{Z_X}$ can be then measured by using the voltage value measured on the "High" point and the value of the voltage across R_r by

$$\overline{Z_X} = \frac{\overline{V_X}}{\overline{I_X}} = -R_r \frac{V_x}{V_r}, \tag{2.34}$$

In practice, the configuration of this method differs for each type of instrument and because of that, there are disadvantages that prejudice the system quality. For instance, LCR meters in a low frequency range bellow 100 kHz, which employ a simple operational amplifier for I-V conversion, present a low accuracy for higher frequencies mainly due to the operational amplifier slew rate.

As for wideband LCR meters and impedance analysers, an I-V converter consisting on an integrator (loop filter), a null detector, a phase detector and a vector modulator to ensure a high accuracy for frequencies reaching over 1 MHz, can execute measures at frequencies ranging from 20 Hz to 110 MHz [14]. This method has the advantage of having a high accuracy over a wide impedance measurement range and the capability of performing a grounded device measurement.

2.5.7 DSP/dsPIC Based

This method is based on the method I-V, explained in section 2.5.3. It consists on measuring the unknown impedance $\bar{Z}$ by using the reference impedance Z_R whose value is well known, and is seen in Figure 2.14.

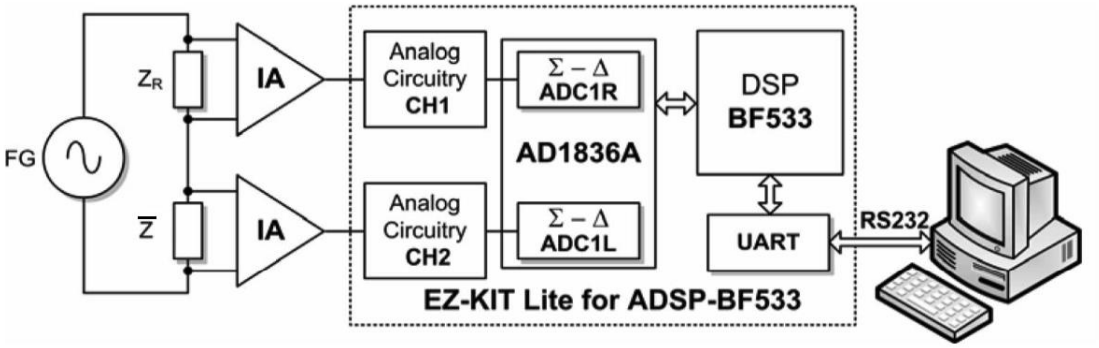

Figure 2.14 - DSP based setup. Taken from [15].

To measure $\bar{Z}$, a function generator (FG) supplies the reference impedance in series with the unknown impedance, two ADCs with differential input, simultaneously sample the voltage across the two impedances, which is then transmitted to the processing unit, the DSP. There, the signal processing, based on the ellipse fitting algorithm, will estimate the sine amplitudes, DC components and phase difference [15].

Instead of using a DSP, a dsPIC can be used, as presented in Figure 2.15. This method was implemented in [16] and later on used by [9] in order to measure viscosity.

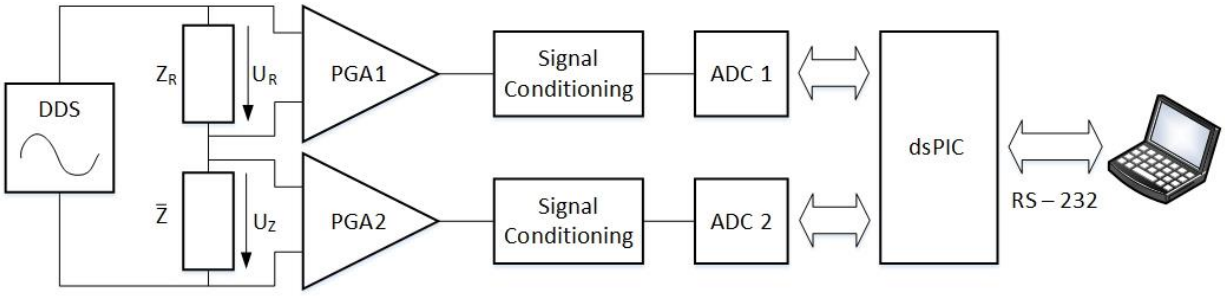

Figure 2.15 - Setup based on a dsPIC. Adapted from [9].

The amplitude of the unknown impedance $\bar{Z}$ can be calculated based on the value of the amplitude of the well-known value reference impedance Z_R, and the amplitudes of the sine signals that run across both impedances. The sine signals are generated by the DDS, which is controlled by the dsPIC via SPI. Since there is no synchronism between the signal generation and acquisition processes, it was required to implement algorithms on both the dsPIC and PC in order to determine the unknown impedance. Contrary to the previous case, instead of implementing the ellipse fitting algorithm[1] on the processing unit, the dsPIC determines the frequency value by implementing IpDFT and FFT algorithms and the amplitude and phase of the unknown impedance are determined by using three and seven sine fitting algorithms on the PC.

2.5.8 Lock-in-Amplifier

[1] Non-iterative method based on Lagrange multipliers.

The Lock-in Amplifier method, presented in Figure 2.16, is used for measuring small AC signals, some down to a few NanoVolts and even when noise sources are higher than the signal of interest, accurate measures can be made. This method is implemented by using a technique called “phase sensitive detection” applied to single out the signal at a specific test frequency. Since this method only measures AC signals near the test frequency, noise signals at other frequencies are ignored, and it also reduces the effects of thermoelectric voltages, both DC and AC.

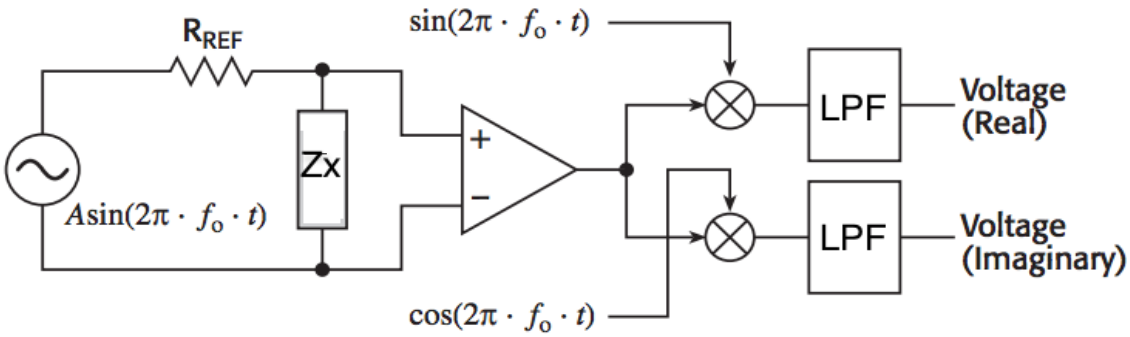

Figure 2.16 - Lock in Amplifier Setup. Taken from [17].

On this method, a current is forced through the unknown impedance $\overline{Z_X}$, by applying a sinusoidal voltage across the resistance R_{REF} in series, which value is well known. The voltage at $\overline{Z_X}$ is amplified and multiplied by both a sine a cosine waves with the same frequency and phase as the applied source and then two low pass filters are applied [17]. This method uses a technic called Quadrature Demodulation which allows the conversion of the signal to a lower IF. The outputs of the low pass filters are called In-Phase (real part) and Quadrature (imaginary part) signals, which after processing, allow the extraction of the amplitude and phase components of the unknown impedance.

2.6 Summary

In this chapter, impedance and viscosity concepts were presented, as well as reference liquids, which are of great importance in order to obtain valid viscosity measurements. Furthermore, an overview of the state of the art concerning viscosity and impedance measurements methods was made. Besides that, some applications involving those methods were presented. The viscosity method, upon which this work is based on, the viscosity wire sensor, was also described in a more detailed way.

3 Architecture

This chapter is divided into three parts. In the first one, an overview of the architectures studied and implemented is made. The second part is focused on the hardware chosen for the system so that the sensor's impedance can be measured. The third part revolves around the algorithms that were studied and that needed to be applied to determine the viscosity.

3.1 System Architecture

The architecture chosen, implemented in [9] and [16] and presented in Figure 3.1 was based on the I-V method described in section 2.5.3, and can be divided into two main parts, signal generation and signal acquisition.

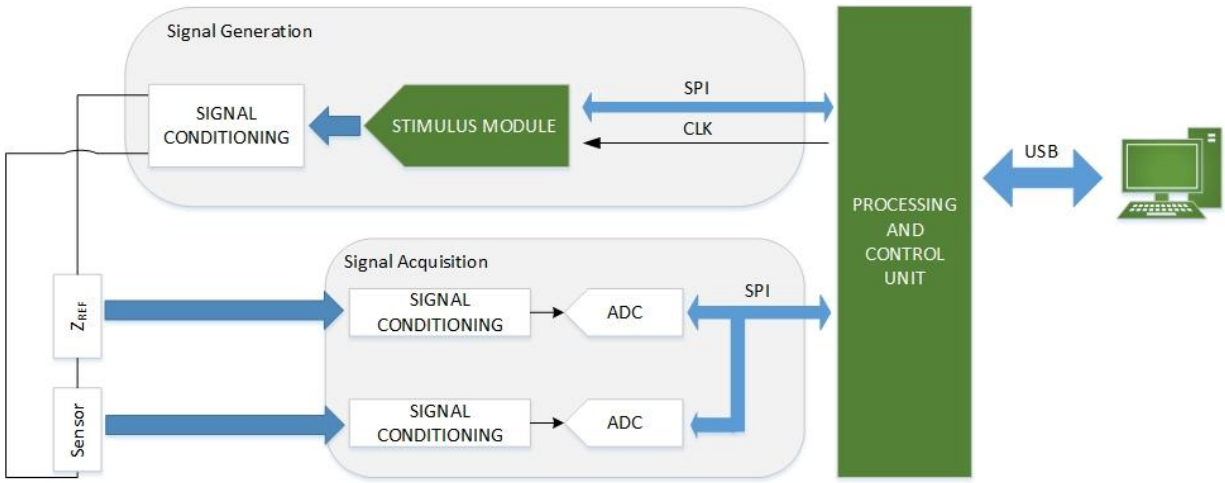

Figure 3.1 - System Architecture.

The signal generation is handled by the stimulus mode, explained further on this report in section 3.2.3, and the main difference when comparing it to the work developed previously is the fact that the frequency reference for the clock is common for both the generation and the signal acquisition. This feature allows a reduction of the processing needed to determine the sensor's impedance, amplitude and phase. Like on the previous work, the stimulus module studied was a DDS, used to generate the required signals.

As for the processing unit, contrary to what was previously implemented, instead of using a dsPIC, was used a DSP, which presents higher processing capabilities, and in this case have the ability to provide clock references to the rest of the system and therefore allowing synchronism. In regards to the signal acquisition, two ADCs, one for each channel were used.

The processing unit, besides controlling both the generation and acquisition system, is also responsible for communicating with a personal computer, and therefore receive commands and send the information that is requested.

3.2 Hardware

The hardware of the system studied and developed is divided into a processing and control unit, a stimulus module, signal conditioning and analog to digital converters, which are approached in this chapter.

3.2.1 Processing and Control Unit

The processing and control unit is a Digital Signal Processor (DSP). Contrary to the previous work [9], mentioned in the second part of section 2.5.7, instead of using a dsPIC a DSP is used, since it presents higher digital signal processing capabilities and therefore allows that all of the processing is accomplished without the need of an external control unit (PC). With that said, besides determining the vibrating wire's sensor impedance, it was intended that the DSP could also be capable of estimating the viscosity of the fluid around the wire. In addition to having improve data processing, the DSP also has a high memory capacity, either internal or through an external RAM module.

Taking into account the capabilities needed and the architecture of the system, the chosen DSP was the ADS-21489 SHARC processor from Analog Devices [18]. It is a processor based on a Super Harvard architecture, which has separate program and data memory, as well as I/O processor and buses, enabling direct interfacing with the processing core and the internal memory. It has 400 MHz core clock speed, features 32-bit fixed and floating-point arithmetic format and comes with 5 Mbits of on-chip RAM, a 16-bit wide SDRAM external memory interface and a DMA engine. It includes multiple communication protocols such as UART, SPI, I^2C and PWM signal generator.

The signal frequency reference clock for the signal generator, as well as the ADCs responsible for acquiring the signal, will be set by the DSP. Because of that, there will be an equal frequency reference for both the generated and acquired signals, allowing the reduction of the processing required in order to determine the unknown impedance of the vibrating wire sensor. Having said that, by taking into account the range of frequencies needed to stimulate the sensor around the resonant frequency, the sampling frequency, as well as the reference clock frequency for the DDS and ADCs, were selected. To know that range, some experimental measurements, presented further on this report in chapter 5.1, were made.

3.2.2 Analog-to-Digital Converter

To implementing this system, two ADCs, as shown in the architecture presented in Figure 3.1, were used. This is required because to measure the impedance, both the sensor and the reference impedance signals must be acquired. Since the DSP chosen only has two serial peripheral interfaces (SPI) and one must be used for the stimulus module, the ADCs were connected on a daisy-chained mode, sharing one of the SPI interfaces.

For this work, it was required to acquire bipolar signals and therefore the ADCs would either have that ability or some previous signal condition allowing the acquisition of unipolar signals. The sampling frequency for the ADCs is dependent of the clock reference frequency that is given by the

DSP and can be defined according to the input signal that is going to be acquired by the ADCs. By ensuring that the Nyquist Theorem is respected and by knowing the sampling frequency, the clock reference frequency is given by

$$f_{clk} = f_{sampling} \times N, \tag{3.1}$$

where N is the number of clock cycles that the ADCs needs to make a conversion. Oversampling may be considered since it will avoid anti-aliasing, as well as increase the resolution and the SNR of the ADCs [19]. However, since the measured frequency is below 10 kHz, it will not be considered.

The ADCs chosen were the AD7988-5, which are 16-bit analog-to-digital converters of successive approximations that operate from a single power supply and offer a max of 500 kSPS throughput [20]. To develop this work two signals must be considered and therefore two ADCs, connected on a daisy chain mode, were used. Because of that, instead of 16-bit samples, 32-bit samples are acquired by DSP. As shown in Figure 3.2, the daisy chain connection consists on sending through one ADC the output of the other, and by that way, the DSP is only required to have a 3-wire connection with the two ADCs, convert, data and clock.

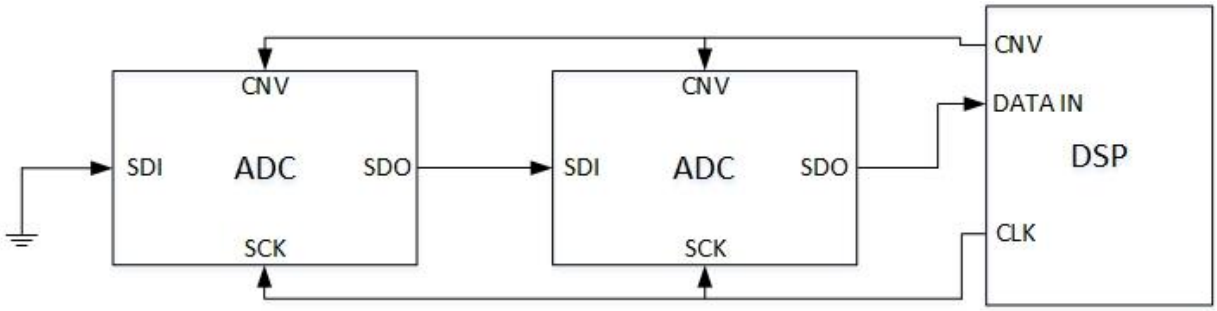

Figure 3.2 - ADCs in daisy chain mode.

Given the fact that the ADCs chosen are unipolar, some signal conditioning was required, which will be explained in section 3.2.4. The ADC reference voltage was set to 2,5V to provide the required resolution for the signals that are acquired.

3.2.3 Stimulus Module

To stimulate the circuit it is required a sinusoidal signal and to do that was decided to use a Direct Digital Synthesizer (DDS). A DDS is a synthesizer that can generate arbitrary waveforms from a fixed clock reference frequency and it works by going through a look-up-table (LUT) with the corresponding waveform samples and by outputting these through a Digital-to-Analog converter (DAC). To be able to do that, the DDS uses digital hardware called numerically controlled oscillator (NCO), which is composed by a phase accumulator, a phase modulator and a high-speed memory.

The DDS presents the samples to the DAC to obtain an analog waveform with the specific frequency structure. The reference clock signal is responsible for controlling the DAC, allowing an output signal with the desired amplitude. Therefore, the output frequency

$$f_{signal} = \frac{Mf_{clk}}{2^N}, \tag{3.2}$$

of the DDS is a function of the system clock frequency, f_{clk}, the number of bits in the phase accumulator, N and the phase increment, M.

The frequency resolution

$$\Delta f = \frac{f_{clk}}{2^N}, \tag{3.3}$$

for the DDS, is a function of the clock frequency, f_{clk}, and the number of bits employed in the phase accumulator, N [21]. Taking advantage of (3.2), the sampling frequency can be chosen as long as the Nyquist Theorem is respected.

Taking into account the previous work developed the DDS chosen was the AD9833, which is a low power, programmable waveform generator capable of producing sine, triangular and square wave outputs [22]. For this work, the DDS was used to generate a sinusoidal signal with the desired frequencies, responsible of stimulating the vibrating wire sensor. The AD9833 can generate signals that vary frequency from 0 Hz to 12,5 MHz.

In Figure 3.3, a sinusoidal signal generated by the DDS, with 1 kHz frequency and an amplitude of 0.6 Vpp, is represented and in Figure 3.4 the correspondent FFT is represented. The measured signal was obtained with the NI USB-6251 from National Instruments, connected to LabVIEW, which is a USB high-speed multifunction DAQ device.

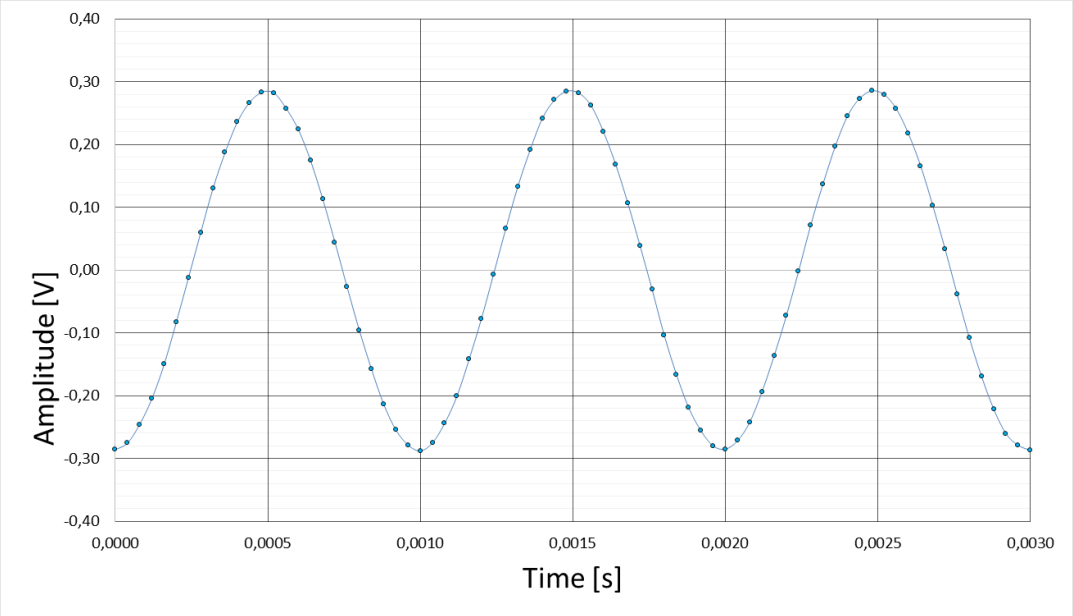

Figure 3.3 - DDS signal with 1 kHz.

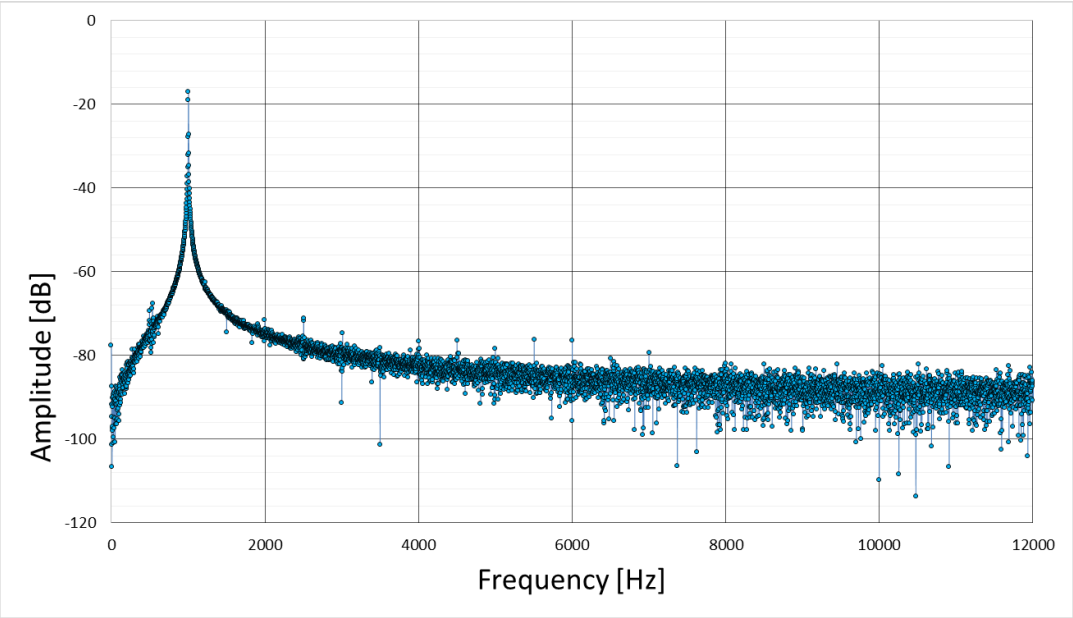

Figure 3.4 - FFT of DDS generated signal.

3.2.4 Signal Conditioning

By observing Figure 3.1, was studied the need of signal conditioning on the signal generated by the stimulus module and on the measured signals that are acquired by the ADCs.

As for the generated signal, it needed to be an AC signal and to insure that happens, a high pass filter was applied. Secondly, since the signal was small, an amplification stage was required, as shown in Figure 3.5.

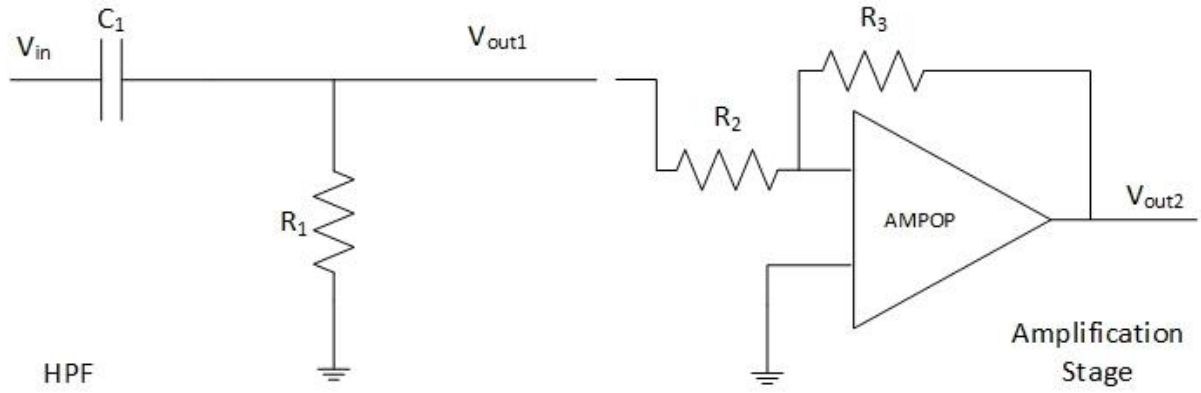

Figure 3.5 - High pass filter and amplification stage.

The cut-off frequency of the filter applied is

$$f_{cut} = \frac{1}{2\pi R_1 C_1} = \frac{1}{2\pi \times 100\text{k}\Omega \times 10\mu\text{F}} = 0.16\ \text{Hz}, \tag{3.4}$$

dimensioned to cut off DC signals. The gain for the amplification stage, which was made with the ADA4891 from Analog Devices [23], can be determined by

$$G = \frac{V_{out1}}{V_{out2}} = -\frac{R_3}{R_2} = -\frac{20\text{k}\Omega}{10\text{k}\Omega} = -2. \quad (3.5)$$

As for the acquired signals by the ADCs, programmable gain amplifiers (PGAs) and operational amplifiers were used. The PGAs present two important functions, increase amplitude of the signals acquired by the ADCs, improve their resolution, as well as the introduction of isolation between the ADCs and the measured impedances. By doing that, the input impedance influence of the ADCs is reduced to a minimum. The operational amplifiers, one for each signal acquired, insure that the signals sent to the ADCs are only positive.

The PGAs chosen were the AD8250 from Analog Devices [24], and give the possibility to choose gains of 1, 2, 5 and 10. They can be controlled digitally by the DSP, making it easy to choose the desired gain. The gain is controlled by switching various internal resistances of the PGAs, which is made by controlling three pins, as shown in Table 3.1. Since the gain of the PGAs only change when $\overline{WR}$ suffers a change in flank, *A1* and *A0* can be shared between the two PGAs, which will reduce the number of pins needed to control them.

Table 3.1 - Truth table for the PGAs gain.

$\overline{WR}$	*A1*	*A0*	*Gain*
1 → 0	0	0	1
1 → 0	0	1	2
1 → 0	1	0	5
1 → 0	1	1	10
0 → 1	X	X	X
0 → 1	X	X	X
1 → 0	X	X	X

The operational amplifiers used were the ADA4891, from Analog Devices, and were implemented in a differential assembly, as shown in Figure 3.6.

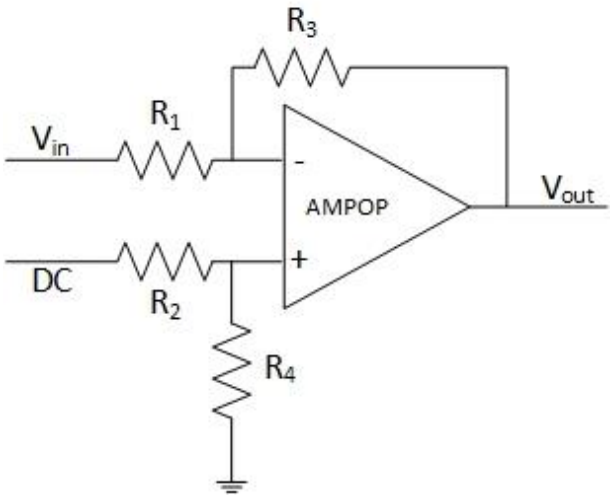

Figure 3.6 - AmpOp in difference assembly.

As for the output voltage, it is given by

$$V_{out} = \frac{R_1 + R_2}{R_1} \times \frac{R_4}{R_3 + R_4} \times DC - \frac{R_2}{R_1} \times V_{in}, \tag{3.6}$$

and since it was dimensioned that

$$\frac{R_1}{R_2} = \frac{R_3}{R_4}, \tag{3.7}$$

the output voltage will be

$$V_{out} = DC - V_{in}. \tag{3.8}$$

This setup not only adds a DC component to the signal, it also inverts it. However, there is no need to rectify the phase difference applied given the fact that it is only intended to determine the phase difference between the two signals acquired. Since they both suffer the same changes throughout the system, the phase difference is the same.

3.2.5 Connection Setup

The connection setup chosen for measuring the signals on the sensor and reference impedance terminals, as well as the connection between the various components of the system, is presented in Figure 3.7.

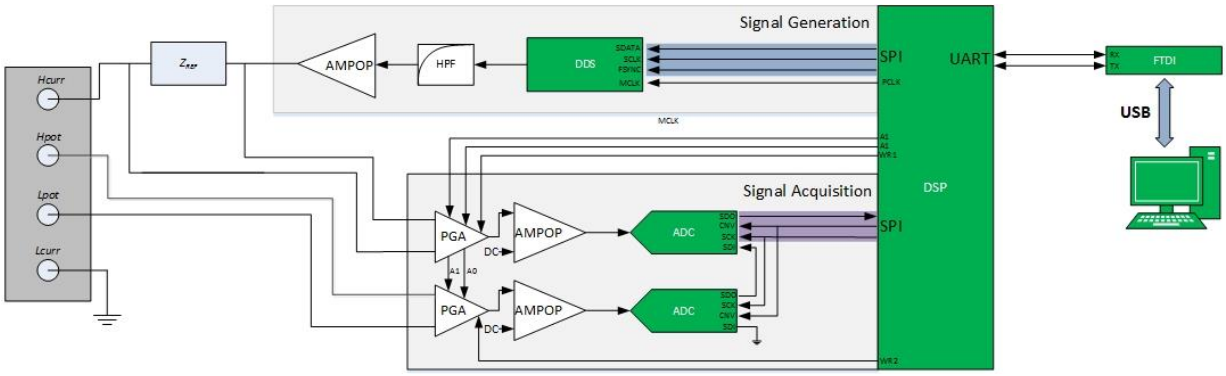

Figure 3.7 - Five Terminal Connection Setup.

By taking advantage of a Din5 connector, a five terminal configuration was used, which is a combination of a three and four-terminal configurations. The four terminals acquired from the sensor, connected to the system acquisition, correspond to the highest and lowest potentials of the current and voltage.

This setup was selected because it reduces the parasitic effects introduced by the cables that make the connection to the measurement circuit, due to the fact that the voltage and current paths are independent [14].

3.3 Algorithms

This chapter is composed by the study of the algorithms needed to be used in the time and frequency domains, as well as the algorithms used to determine the impedance value of the vibrating wire sensor, required to determine the equivalent parameters of the electric model of the sensor.

3.3.1 Frequency Domain

On the frequency domain three different algorithms were initially studied. The IpDFT, the FFT and the Goertzel. The FFT and the Goertzel algorithms are similar, since both transpose the signal sample on the time domain to the frequency domain and therefore allowing to obtain the signal spectrum, used by the IpDFT algorithm.

Contrary to the FFT that always computes all the frequency components and most of them are discarded, as they present no interest, the Goertzel algorithm is specialized in computing a subset of output frequencies [25][26].

The basic relation of the discrete Fourier transform is

$$X[k] = \sum_{n=0}^{N-1} x[n] e^{-j2\pi n \frac{k}{N}}, \tag{3.9}$$

where $x[n]$ is a discrete signal of length N and $X[k]$ is a k^{th} bin of the Fourier spectrum. Function (3.9) can be put into a convolution form

$$y_k[n] = \sum_{n=-\infty}^{\infty} x[n] e^{j2\pi(m-n)\frac{k}{N}} u[m-n]. \tag{3.10}$$

An impulse response of the derived filter is then a complex harmonic signal

$$h(n) = e^{j2\pi \frac{k}{N}}, \tag{3.11}$$

of which length is constrained by a rectangular window. By applying the Z-transform[1] to the impulse response (3.11), it is possible to find the transfer function of the Goertzel filter

$$H(z) = \sum_{n=0}^{\infty} h(n) z^{-1} = \frac{1}{1 - z^{-1} e^{j2\pi \frac{k}{N}}}, \tag{3.12}$$

whose modified form is

[1] Converts a discrete-time signal into a complex frequency domain representation.

$$H(z) = \frac{1 - z^{-1}e^{-j2\pi\frac{k}{N}}}{1 - 2z^{-1}\,cos\left(2\pi\frac{k}{N}\right) + z^{-2}}, \tag{3.13}$$

which can be split into the real recursive and the complex direct computational parts, turning it more convenient for the implementation of the Goertzel algorithm. The realization of the transfer function (3.13) is shown in Figure 3.8

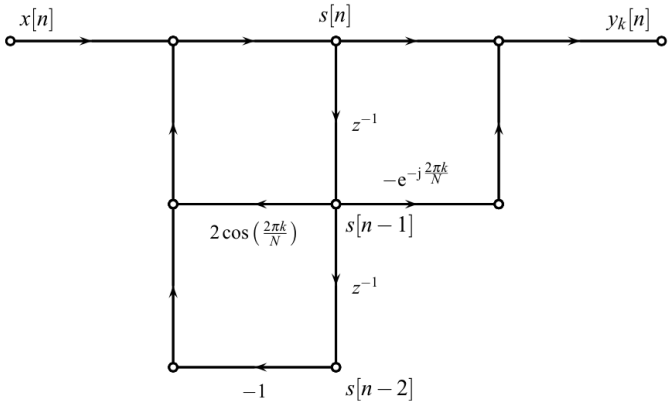

Figure 3.8 - Goertzel Filter. Taken from [25].

Since there will be synchronism between the generation and acquisition of the signals, the implementation of the Goertzel algorithm will bring benefits in terms of memory and a faster processing.

The IpDFT is used to determine with accuracy the signal's frequency, by searching the spectrum, obtained with the Goertzel, for the biggest element and the ones that are adjacent to it [27] and because of that, two situations can occur. First, if the larger neighbour is on left side of the maximum element, $X(L)$ corresponds to the larger neighbour and $X(L+1)$ to the maximum element. Secondly, if the larger neighbour is on the right side of the element, $X(L+1)$ corresponds to the larger neighbour and $X(L)$ to the maximum. Each value in the frequency domain is a complex number composed by a real and imaginary part,

$$X(L) = U_L + jV_L \tag{3.14}$$

and

$$X(L+1) = U_{L+1} + jV_{L+1}. \tag{3.15}$$

It is possible to measure the signal's frequency by applying

$$f = \lambda \Delta f, \tag{3.16}$$

where Δf is the spectrum's resolution, in other words the sampling frequency, and λ is given by

$$\lambda = \frac{arcos\left(\frac{Z_2 cos\big(n(L+1)\big) - Z_1 cos(nL)}{Z_2 - Z_1}\right)}{n}, \tag{3.17}$$

with

$$Z_1 = V_L\left(\frac{k_{opt} - cos(nL)}{sin(nL)}\right) + U_L, \tag{3.18}$$

$$Z_2 = V_{L+1}\left(\frac{k_{opt} - cos(n(L+1))}{sin(n(L+1))}\right) + U_{L+1}, \tag{3.19}$$

$$k_{opt} = \frac{\big((sin(nL))(V_{L+1} - V_L) + (cos(nL))(U_L + U_{L+1})\big)}{U_{L+1} - U_L}, \tag{3.20}$$

and

$$n = \frac{2\pi}{N}, \tag{3.21}$$

whose *N* is the number of samples [28].

3.3.2 Time Domain

In the time domain, sine fitting algorithm of three parameters [29], was studied. Sine fitting algorithms are implemented when there is the need to obtain a set of parameters corresponding to the analytical expression of a sine signal, while minimizing the sum of the squared errors between the estimated parameters and the acquired samples. Given that, the implementation of these algorithms will allow determining with great accuracy the amplitude and phase of the acquired signals.

The three-parameter sine-fitting algorithm is a non-iterative algorithm that can estimate the amplitude, phase and DC component of an acquired sine wave of known frequency, which in this case was determined by the Goertzel algorithms, with a certain sampling frequency. The acquired sine signals can be represented by

$$u(t) = Dcos(2\pi ft + \emptyset) + C = Acos(2\pi ft) + Bsin(2\pi ft) + C, \tag{3.22}$$

where

$$D = \sqrt{A^2 + B^2}, \tag{3.23}$$

and

$$\emptyset = -atan2(B, A). \tag{3.24}$$

In (3.24), the function $atan2$ is a variation of $arctan$ that takes into account the signs of both vector components (B and A), and places the angle in the correct quadrant considering all four quadrants [16].

To measure parameters A, B and C, the algorithm starts by creating a matrix with three columns and N lines, that correspond to the number of samples acquired,

$$M = \begin{bmatrix} cos(2\pi f t_1) & sin(2\pi f t_1) & 1 \\ \vdots & \vdots & \vdots \\ cos(2\pi f t_N) & sin(2\pi f t_N) & 1 \end{bmatrix}. \tag{3.25}$$

After that, the parameters are estimated through the parameter vector

$$\hat{x} = [A \quad B \quad C]^T, \tag{3.26}$$

which is given by

$$\hat{x} = M^{\dagger} y, \tag{3.27}$$

where y is the sample vector and $M^{\dagger}$ the pseudo inverse matrix of *M* [30][31].

3.3.3 Impedance Measurement

To estimate the viscosity of the fluid involving the vibrating wire sensor, it is required to measure its impedance and after that proceed to the determination of the parameters needed to determine viscosity. Therefore, to measure the impedance of the sensor, it is required to know the magnitude and phase of the signals passing through the sensor and reference impedance. Considering the circuit in Figure 3.7, presented in section 3.2.5, amplitude and phase angle of the impedance under measurement are calculated by

$$|\bar{Z}| = |Z_{Ref}| \frac{|U_{Sensor}|}{|U_{Ref}|} \tag{3.28}$$

and

$$\emptyset = \phi_{Z_{Ref}} + \left(\phi_{U_{Sensor}} - \phi_{U_{Ref}}\right). \tag{3.29}$$

3.3.4 Sensor Equivalent Parameters Measurement

To estimate the parameters that model the electric circuit of the sensor, it is required to adapt the frequency response of sensor, to the complex impedance described by (2.17). This fit is made by finding the parameters of the circuit that minimize the cost function

$$\varepsilon = \sum_{i=1}^{M} \sqrt{\left(\Re\left(Z_{T_i}\right) - \Re(Z_{m_i})\right)^2 - \left(\Im\left(Z_{T_i}\right) - \Im(Z_{m_i})\right)^2}, \tag{3.30}$$

where Z_{T_i} corresponds to the value of the impedance given by (2.17), for a frequency ω_i, Z_{m_i} corresponds to the value of impedances measured and M to the number of frequency values [9].

To minimize the cost function (3.30), it was needed to implement on the DSP the MATLAB function named *fminserch*[1],that looks for the minimum value of a function. The algorithm receives the impedance values measured and returns the parameters R_s, L_s, C, L_p and G that minimize the distance between the experimental and theoretical responses. To be able to work, the function requires an initial value for the parameters that need to be determined.

3.4 Summary

In this chapter, the chosen system architecture, methodology to develop it and the algorithms studied, were described. In the hardware section was approached the processing and control unit, the DSP, responsible for communicating with the signal generator module needed to stimulate the vibrating wire sensor, with the two ADCs, responsible for performing signal acquisition, as well as with the personal computer who will be responsible for sending commands and expose results to the user. To ensure that there is a synchronism between signal acquisition and generation, the reference clock frequency for both the ADCs and for the signal stimulus module were from the DSP. This feature, allows a reduction of the required processing capabilities. As for the algorithms studied, to determine the impedance of the vibrating wire sensor, was studied the Goertzel, IpDFT and three parameter sine-fitting algorithms.

[1] Finds the minimum of a scalar function of several variables, starting at an initial estimate.

4 System Software

On this chapter, the software developed in the DSP, as well and the LabVIEW program for the user to communicate with the system, is approached. The software for the DSP provides the communication between all the hardware modules and LabVIEW allows the user to set parameters, inspect variables and acquired measurements.

During this work, the ADSP-21369 EZ-KIT Lite was used, which is an evaluation system designed to be used with the VisualDSP++ development environment to test the capabilities of the ADSP-21369 SHARC processor [32].

4.1 USB Communication

To communicate between the PC and the DSP, USB protocol was implemented. This was done by using an integrated circuit, the FT232RL, from Future Technology Devices International Ltd, which allows the interface between the UART module of the DSP and the USB from the PC.

Given the fact that the UART module only transmits 8 bits at a time, some processing, was required, not only to the data sent to the PC, but also to the commands sent to the DSP. Since it is a controlled system, both of them are well known and therefore the software developed took that into account.

In regards to the commands sent to the DSP, they are pre-configured, which means that the user can only communicate with the DSP by recurring to a fixed number of commands, which will be explained in section 4.3 of this report.

As for the information sent to the PC, besides the need of some processing by the DSP, as previously said, it was required that the data sent was encoded in a manner that the PC could read it, due to the fact that the same rules, used in the commands, needed to be followed.

4.2 SPI Communication

4.2.1 DDS and DSP

The communication between the DDS and the DSP was made using the SPI protocol, since the DDS is written to via a three-wire serial interface, as shown in Figure 4.1.

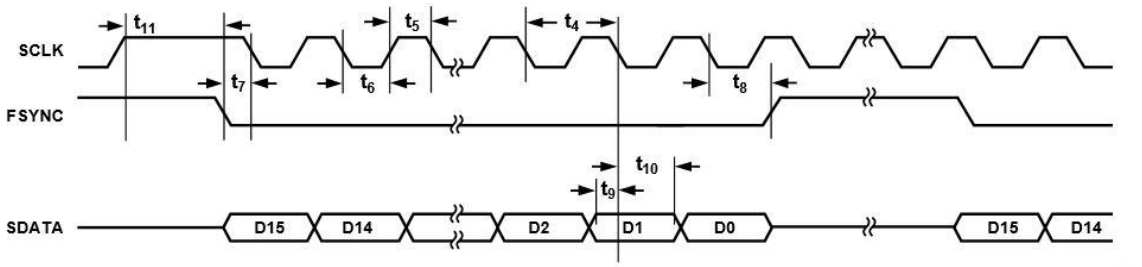

Figure 4.1 - DDS temporal diagram for SPI communication. Taken from [22]

With that said, the communication between the DDS and the DSP is only in write mode, which means there is only data transmitted from the DSP to the DDS, and therefore the DSP must send the needed word sequence so that the wanted frequency is generated.

To insure that the reference frequency between the signal generated and the signal acquired was maintained, the clock signal used on the DDS was created by the DSP. Therefore, besides the clock signal, when the DSP writes to the DDS, it is implemented the SPI interface. The SPI communication needs to insure that besides the word sequence to generate the frequency wanted, sent to SDATA, it is also created the SPI clock signal, sent to SCLK and that the FSYNC terminal changes flank from high to low between words.

The command sequence sent to the DDS is composed of five words, as shown in Table 4.1. The first word resets the registers to zero, which corresponds to an analog output of midscale, the second two words correspond to the frequency wanted, which contain the fourteen less significant bits and the fourteen most significant bits, the forth word contains the phase of the signal and the last one the exit reset. The two words sent in order to get the wanted frequency are calculated by

$$f_{register} = \frac{f_{signal} \times 2^{28}}{f_{clk}}, \tag{4.1}$$

where f_{signal} is the frequency wanted and f_{clk} the clock signal for the DDS [33]. By choosing f_{clk}, the resolution of the DDS is set and can be determined by

$$f_{signal} = \frac{f_{clk}}{2^{28}}, \tag{4.2}$$

Table 4.1 is an example of the word sequence sent to the DDS, in order to obtain a signal of 1 kHz, by having a clock signal of 500 kHz, and therefore a resolution of 0,001 Hz.

Table 4.1 - Word sequence example for DDS.

Register	Hexadecimal	Binary
Control Register	0x2100	0010000100000000
Frequency Register LSB	0x7127	0111000100100111
Frequency Register MSB	0x4020	0100000000100000
Phase Register	0xC000	1100000000000000
Exit Reset	0x2000	0010000000000000

The clock signal generated by the DSP is presented in Figure 4.2, and in this case has a frequency of approximately 500 kHz. To create the needed clock, was used the 32 MHz oscillator from the ADSP-21369 EZ-KIT Lite base clock.

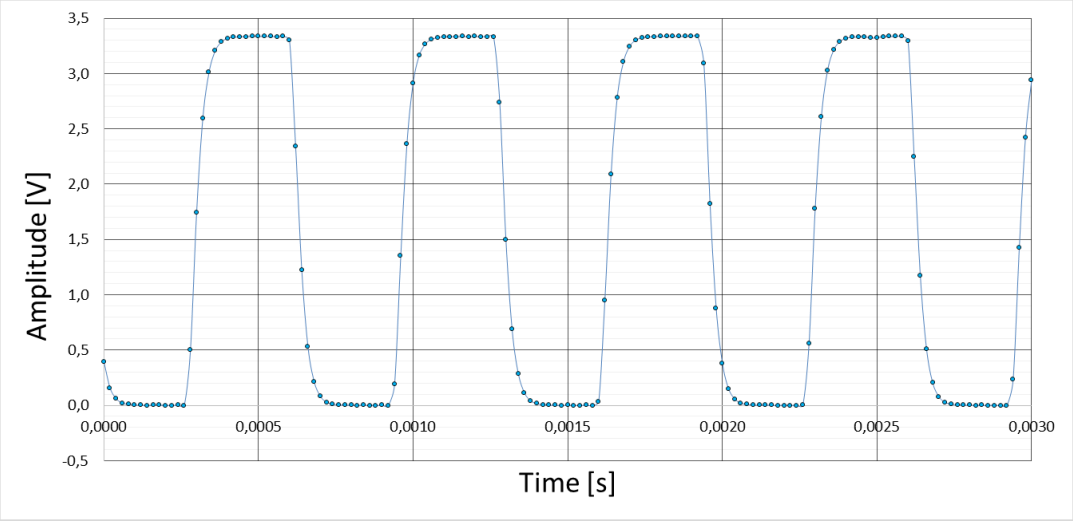

Figure 4.2 - Clock generated for the DDS

The PCG interface of the DSP allows the generation of accurate low-jitter clock signals, synchronized with the core clock.

4.2.2 ADCs and DSP

The communication between the ADCs and the DSP was made by using the SPI protocol on a daisy chain connection, as previously said. To acquire the samples on the ADCs, an interruption that creates the SCK signal, was generated.

As shown in Figure 4.3, by changing the flank of CNV, the conversion of the acquired signals starts. When it finishes, the MSB is placed on SDO and the ADCs start another acquisition. Since it is used a daisy-chain connection mode and since each ADC generates words of 16 bits, 32 clock flanks are required to acquire all bits.

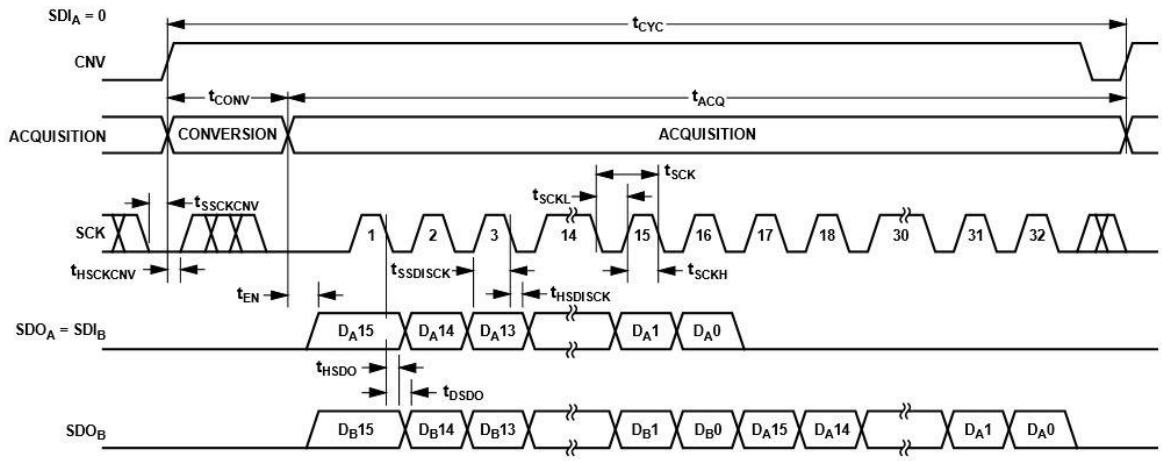

Figure 4.3 - ADCs temporal diagram for SPI communication. Taken from [20].

4.3 Control Program

The control program to communicate with the DSP, presented in Figure 4.4, was developed in LabVIEW, so that the user could execute it from a personal computer. The interface allows the user to get specific values that characterize the system, make a sweep in frequency, save values and run a specific command, like for example make a single acquisition.

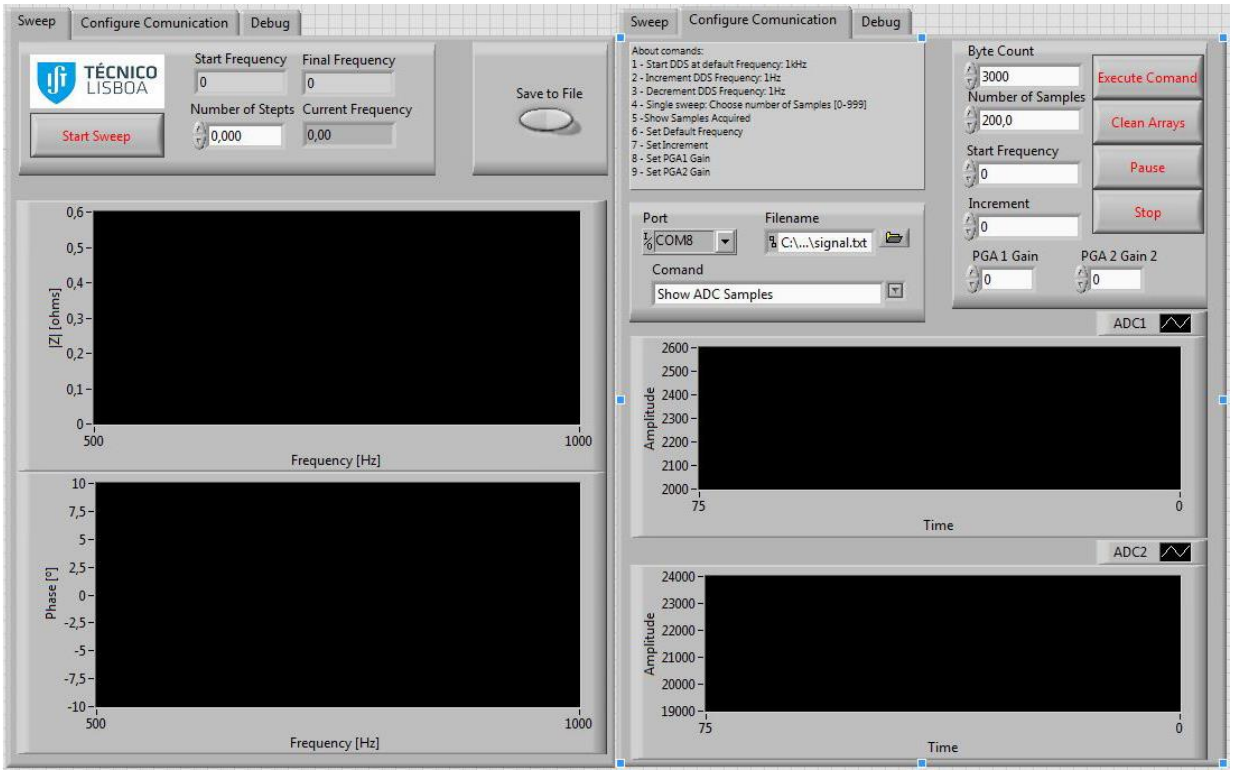

Figure 4.4 - LabVIEW Interface.

It was also given the possibility to configure the PGAs, set the starting frequency of the DDS, as well as the step used when performing the frequency sweep.

The flowchart shown in Figure 4.5, represents the main function of the system developed, the frequency sweep, which was developed by executing a set of commands, such as setting the DDS frequency and acquired the samples from the ADCs.

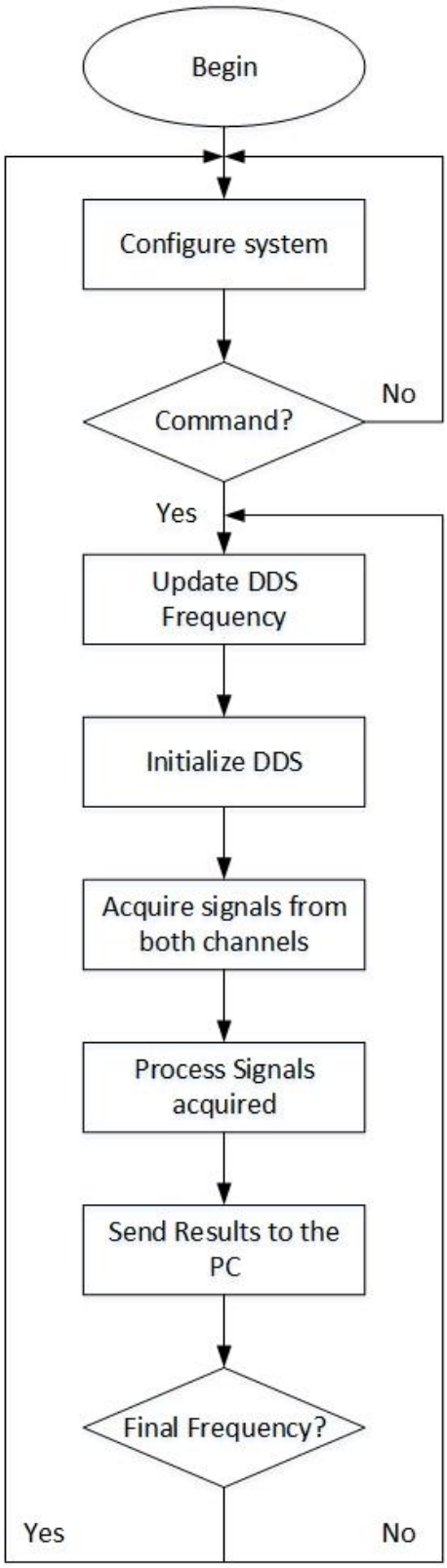

Figure 4.5 - Flowchart of the LabVIEW program developed.

4.4 Summary

In this chapter, the communication protocols implemented were described. To communicate with both the ADCs and the DDS, was implemented the SPI protocol and was required to generate a clock signal for the DDS. As for the communication with the personal computer, was implemented the USB protocol. Lastly, the control program, developed in LabVIEW, was presented and described.

5 Results

5.1 Experimental Results with HIOKI

To determine the range of frequencies upon which the vibrating wire sensor works and study its impedance behaviour when submitted to fluids with different viscosity values, a set of samples, presented in Table 5.1, were made.

Table 5.1 - Samples Tested with HIOKI.

Sample	Water [%]	Glycerine [%]	Viscosity [mPa.s] at 20° C
1	100	0	1,005
2	50	50	6,000
3	25	75	35,500

The sensor's responses to these samples, whose viscosity values were taken from [34], are presented from Figure 5.1 to Figure 5.3, and were obtained with the 3522-50 LCR HiTESTER from HIOKI [35], by making a sweep around the resonance frequency, using the GPIB interface, commanded by a computer running LabVIEW.

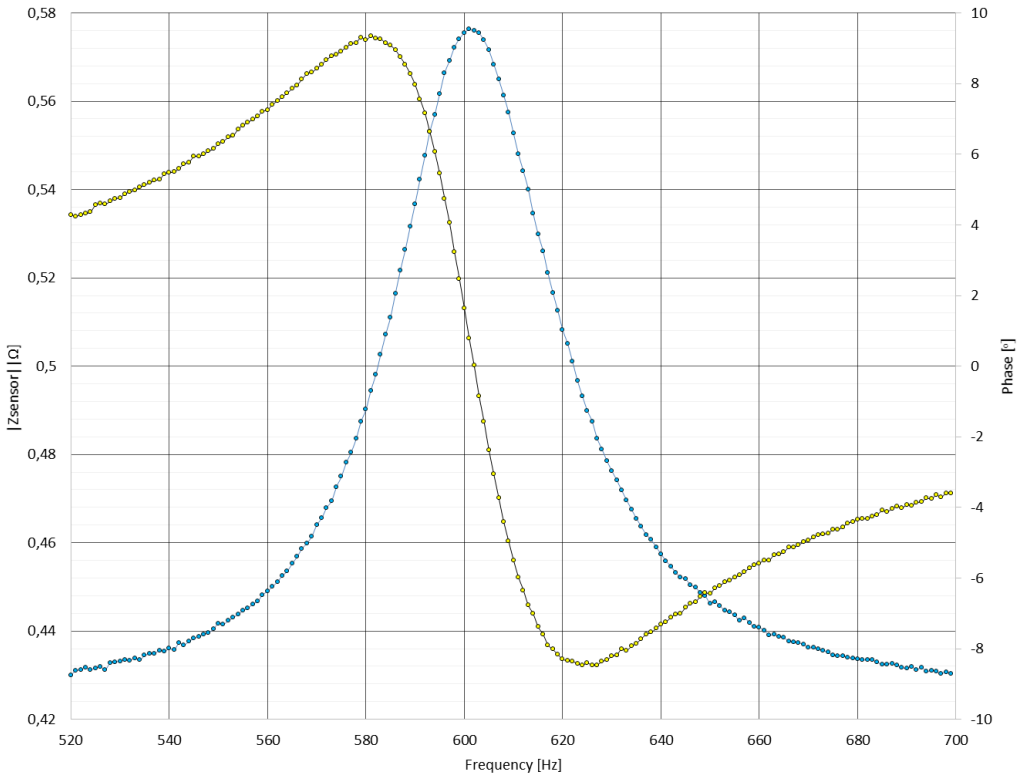

Figure 5.1 - Sensor Frequency Response to sample 1.

Blue - $|Z_{sensor}|$ and Orange - Phase.

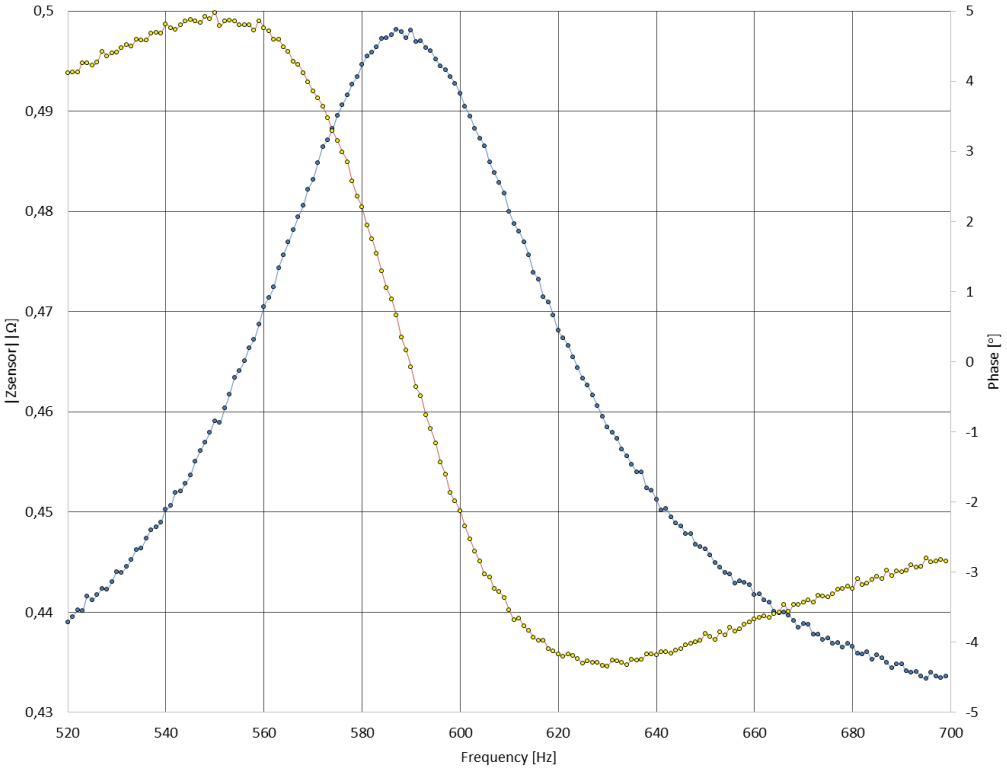

Figure 5.2 - Sensor Frequency Response to Sample 2.

Blue - $|Z_{sensor}|$ and Orange - Phase.

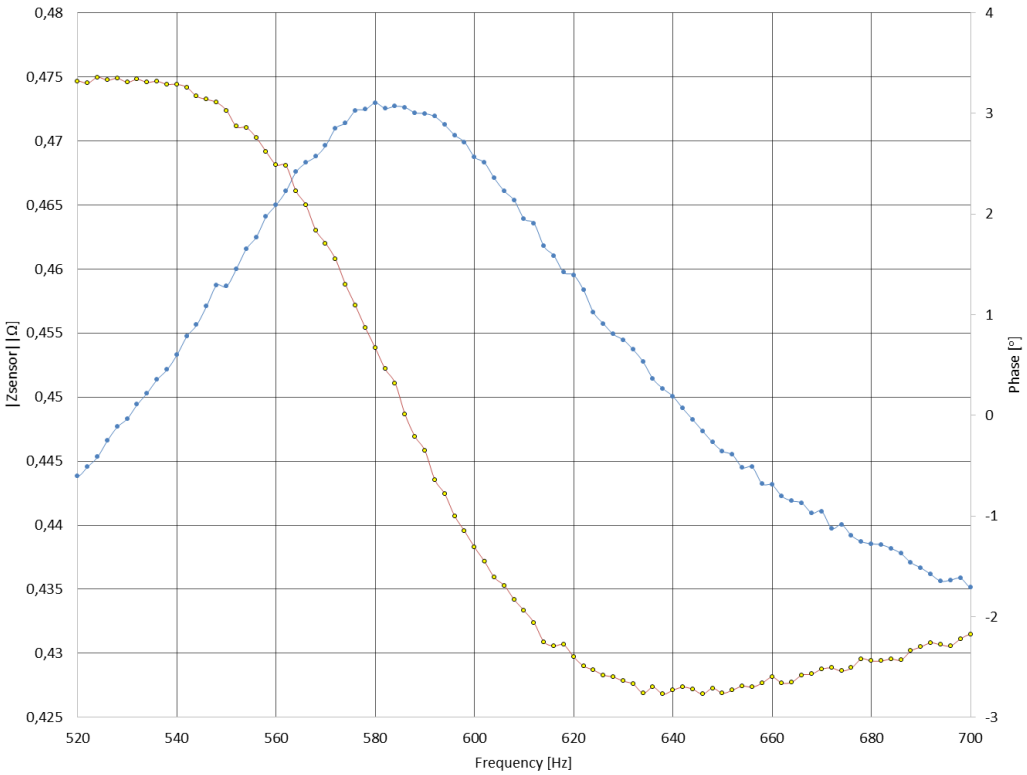

Figure 5.3 - Sensor Frequency Response to Sample 3.

Blue - $|Z_{sensor}|$ and Orange - Phase.

By observing the sensor's responses to the three samples, it is concluded that the resonance frequency varies and it is inside an interval of frequencies that ranges from 500 Hz to 700 Hz. Table 5.2 contains the parameters obtained for the various samples, such as resonance frequency and maximum impedance.

Table 5.2 - Sensor Frequency Response Parameters for the various Samples.

Sample	F_R [Hz]	Z_{MAX} [Ω]
1	602	0,5761
2	588	0,4979
3	586	0,4726

Analysing the values in Table 5.1 and the results presented in Table 5.2, it can be concluded that the resonance frequency F_R and maximum impedance Z_{MAX} decrease with the increase of viscosity. Also, the range of frequencies, for fluids with higher viscosities, will have to be bigger since impedance and phase values have small variations when compared to fluids with lower viscosities.

During the experiments presented, temperature was not controlled, which could imply variations in the viscosity values that were not taken into account.

5.2 System developed

All the modules of the system, except for the processing and control unit, were integrated in the 2-layer PCB, represented in Figure 5.4. As shown in the Figure 5.4, the board developed does not include the DSP, but is composed mainly by the FTDI, DDS, ADCs, Din5 connector, as well as the signal conditioning required for the signal acquisition. The system footprint is 70 mm x 37 mm.

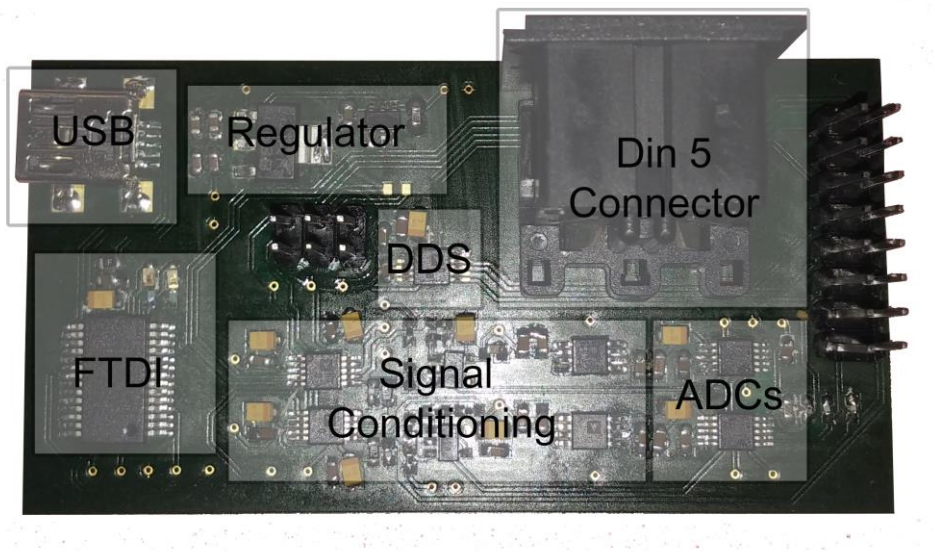

Figure 5.4 - Hardware system without DSP

5.3 Summary

In this chapter, some experiments, with the vibrating wire sensor, were described. The experimental results obtained show that the range of frequencies upon which the signal generation needed to work was between 400 Hz and 1 kHz and therefore, the signal generator and the ADCs were chosen by taking that into account. As for the impedance of the sensor, its value when under the influence of glycerine and water samples, ranges from 0.4 to 0.6 Ω, which will influence the value of the reference impedance chosen. Besides the experimental results, was also described the PCB developed.

6 Conclusion

The main objective of this work was to characterize, implement and develop a system capable of measuring impedances and determine viscosity. For that, the frequency response of the vibrating wire sensor was studied so that the parameters required to analyse viscosity variations could be determined.

In this document several viscosity measurement methods were studied, as well as impedance measurement methods. Viscosity is a characteristic quite important, in order to know how a liquid material will behave and it is of great importance in various technological and industrial areas. The impedance measurement method used and developed, was chosen in order to be portable and low cost, which would not be possible with a device such as HIOKI[1]. Therefore an architecture based on the I-V impedance measurement method was implemented and in this document different parts of the system, that revolve around signal generation and acquisition, were described. Also, the software and algorithms developed and studied, as well as the experiments made to determine the vibrating wire sensor behaviour, were described.

The system architecture was represented and described, as well as the LabVIEW interface developed to perform the communication between the system and the user. The developed system was designed so that it would be possible to connect it to the viscosity sensor and acquired samples from it, when stimulated by the sinusoidal signal, also generated by the system. The processing and control unit, the DSP, was implemented so that the system could receive commands and send information to the personal computer. Therefore, the LabVIEW program allows the user to configure the system, in order to set the systems conditions depending on the vibrating wire sensor behaviour.

It is important to state that the system developed remained unfinished since it did not include the processing and control unit in the final PCB. As mentioned in section 4, was used the evaluation system ADSP-21369 EZ-KIT Lite from Analog Devices, and the final footprint of the system without the DSP, was 70 mm x 37 mm.

In section 5.1, some experimental results obtained with HIOKI, were presented and was intended to use them as a reference and compare them with the system developed. Unfortunately, due to shortage of time and problems encountered in the final PCB, was not possible to acquire the results needed to compare with the experimental results previously obtained. Having said that, it was not possible to test the final PCB developed, however, as was shown during this document, the intermediate PCBs developed, with the different modules of the system, showed that it was possible to create the required control signals with DSP, and therefore maintain the synchronism between the signal generated and signals acquired.

In regards to the algorithms studied, the Goertzel algorithm was tested in MATLAB and developed in C language. However it was not possible to implement it in the DSP, as well as the IpDFT and the sine fitting of three parameters.

[1] Costs approximately 5000 €.

7 Future Work

As mentioned in section 6, the developed system is yet to be concluded. Therefore, the future work suggested is the development of a system that includes the DSP, as well as the other modules. Besides that, it is also required to implement the required algorithms to determine precise values of impedance from the vibrating wire sensor, needed in order to determine viscosity.

There would still be the need of a personal computer running LabVIEW, so that the user could communicate with the system. Therefore, an interesting improvement to the system would be giving it some sort of mobility, by adding a tablet capable of running the required software, and a battery so that it could be used if an environment where a wall socket could not be found.

8 References

[1] L.F.F. Regada, “The Measure of Viscosity of Liquids with a Vibrating Wire Cell,” Instituto Superior Técnico, 2012.

[2] C.A.N. Castro, F.J.V. Santos, J.M.N.A Fareleira, and W.A. Wakeman, “Metrology of Viscosity: Have We Learned Enough? ", in *Journal of Chemical & Enginneering Data*, vol. 54, pp. 171–178, Feb. 2009.

[3] F.J.P. Caetano, “Viscosimetria de Líquidos Novos Fluidos de Referência.”, Instituto Superior Técnico, PhD Thesis.

[4] A.A.H. Pádua, J.M.N.A Fareleira, J.C.G. Calado, and W.A. Wakeman, “Electromechanical model for vibrating-wire instruments,” in *Rev. Sci. Instrum.*, vol. 69, no. 6, pp. 2392–2399, 1998.

[5] S.P Sutera, and R.Skalak, "The History of Poiseuille's,” 1993.

[6] J. Wilke, H. Kryk, and D. Wagner, “Theory and Praxis of Capillary Viscometry".

[7] K.D. Antoniadis, M.J. Assael, and W.A. Wakeman, “Transport Properties of Fluids".

[8] S.A. Shearer, and J.R. Hudson, ’ Fluids Mechanis. Stokes' Law and viscosity”.

[9] N.M.R.F Santos, “Sistema de Medida de Impedâncias baseado num dsPIC para um Sensor de Viscosidade”, Instituto Superior Técnico, Master's Thesis, 2010.

[10] C.J. Schaschke, “High Pressure Viscosity Measurement with Falling Body Type Viscometers,” vol.2, no. 5, pp. 564–576, 2010.

[11] R.A. Secco, J.R. Bruyn, and M.Kostic, “Fluid Viscosity Measurement”.

[12] F.M. Janeiro, P.M. Ramos, J.M.N. Fareleira, J.C.F. Diogo, D.R.C. Máximo, and F.J.P. Caetano, “Impedance spectroscopy of a vibrating wire for viscosity measurements,” in *I2MTC, Boston*, pp. 1067–1072, 2010.

[13] T.Retsina, S. M. Richardson, and W. A. Wakeham, “The Theory of a vibrating rod viscometer", in *Applied Scientic Research,* pp. 325-246, 1987.

[14] Agilent Technologies, “The Impedance Measurement Handbook - A guide to measurement technology and techniques.”, 2000.

[15] P. M. Ramos, F. M. Janeiro, M. Tlemçani, and A. C. Serra, “Implementation of a DSP Based Impedance Measurement Instrument Using Ellipse Fitting Algorithms,” in *IEEE Transactions on Instrumentations and* Measurements, vol. 57, no. 8, pp. 1661-1669,2008.

[16] J.C.S.M. Santos, “Impedance Measuring System based on a dsPIC.", Instituto Superior Técnico, Master's Thesis, 2009.

[17] A. Daire, W. Goeke, and M. A. Tupta, “New Instruments Can Lock Out Lock-ins”, Keithley Instruments, no. 2667, 2005.

[18] Analog Devices, "ADSP-21489 Datashee", March 2013. [Online]. http://www.analog.com/static/imported-files/data_sheets/ADSP-21483_21487_21488_21489.pdf.

[19] Atmel, "Atmel AVR127 : Understanding ADC Parameters.", 2013.

[20] Analog Devices, "AD7988-1/AD7988-5 PulSAR ADCs DataSheet", 2014. [Online] http://www.analog.com/media/en/technical-documentation/data-sheets/AD7988-1_7988-5.pdf.

[21] Analog Devices, "A Technical Tutorial on Digital Signal Synthesis," 1999.

[22] Analog Devices, "AD9833 Programmable Waveform Generator DataSheet", 2012. [Online] http://www.analog.com/media/en/technical-documentation/data-sheets/AD9833.pdf.

[23] Analog Devices, "ADA4891 Rail-to-Rail Amplifiers DataSheet", 2015. [Online] http://www.analog.com/media/en/technical-documentation/data-sheets/ADA4891-1_4891-2_4891-3_4891-4.PDF.

[24] Analog Devices, "AD8250 Programmable Gain Instrumentation Amplifier DataSheet", 2013. [Online] http://www.analog.com/media/en/technical-documentation/data-sheets/AD8250.pdf.

[25] P. Sysel, and P. Rajmic, "Goertzel algorithm generalized to non-integer multiples of fundamental frequency," in *Journal on Advances in Signal Processing.*, 2012.

[26] F. Záplata, "Using the Goertzel algorithm as a filter", no. 3, pp. 14–16, 2014.

[27] K. Duda, "Interpolation Algorithms of DFT for Parameters Estimation of Sinusoidal and Damped Sinusoidal Signals," 2010.

[28] T. Bilau, T. Megyeri, and A. Sárhegyi, "Four-parameter fitting of sine wave testing result: iteration and convergence," *Compututer Standards and Interferances,* vol. 26, pp. 51–56, 2004.

[29] P. M. Ramos, F. M. Janeiro, and T. Radil, "Comparison of impedance measurements in a DSP using ellipse-fit and seven-parameter sine-fit algorithms," *Meas. J. Int. Meas. Confed.*, vol. 42, no. 9, pp. 1370–1379, 2009.

[30] P. M. Ramos and A. Cruz Serra, "A new sine-fitting algorithm for accurate amplitude and phase measurements in two channel acquisition systems," *Measurement*, vol. 41, no. 2, pp. 135–143, Feb. 2008.

[31] P. Handel, "Evaluation of a Standardized Sine Wave Fit Algorithm".

[32] ADSP-214xx SHARC Processor Hardware Reference, Revision 1.0, Analog Devices, February 2012.

[33] L. Riordan, "Programming the AD9833/AD9834" pp. 1–4, Analog Devices, 2010

[34] J.B. Segur, and H.E. Oberstar, "Viscosity of Glycerol and Its Aqueous Solutions," The Miner Laboratories, Chicago,1951.

[35] "HIOKI 3522-50 LCR Instruction Manual", HIOKI E.E.Corporation, 2006.

9 Appendices

A - PCB Developed

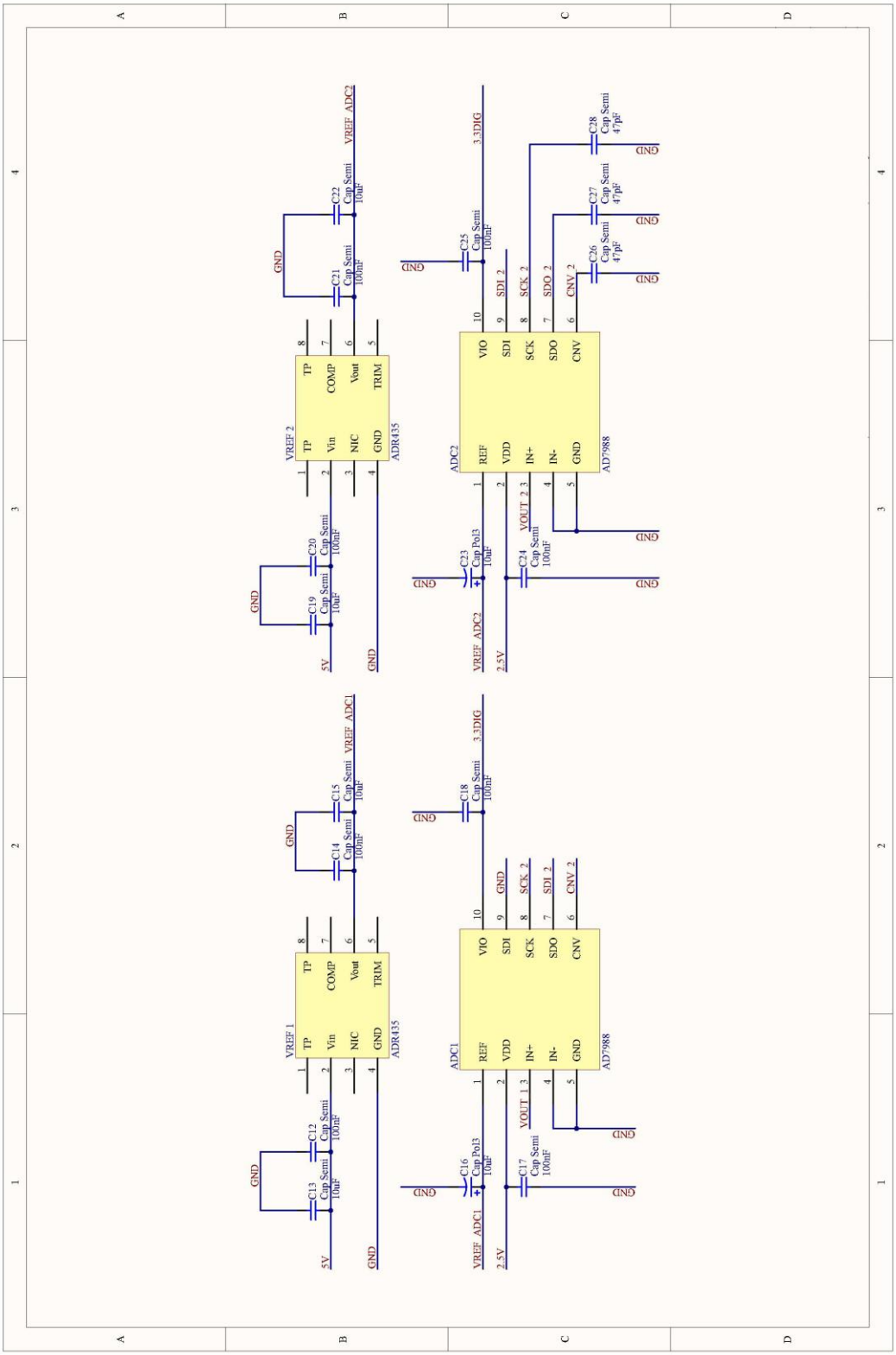

Figure 9.1 - ADCs Electrical schematic and respective voltage reference.

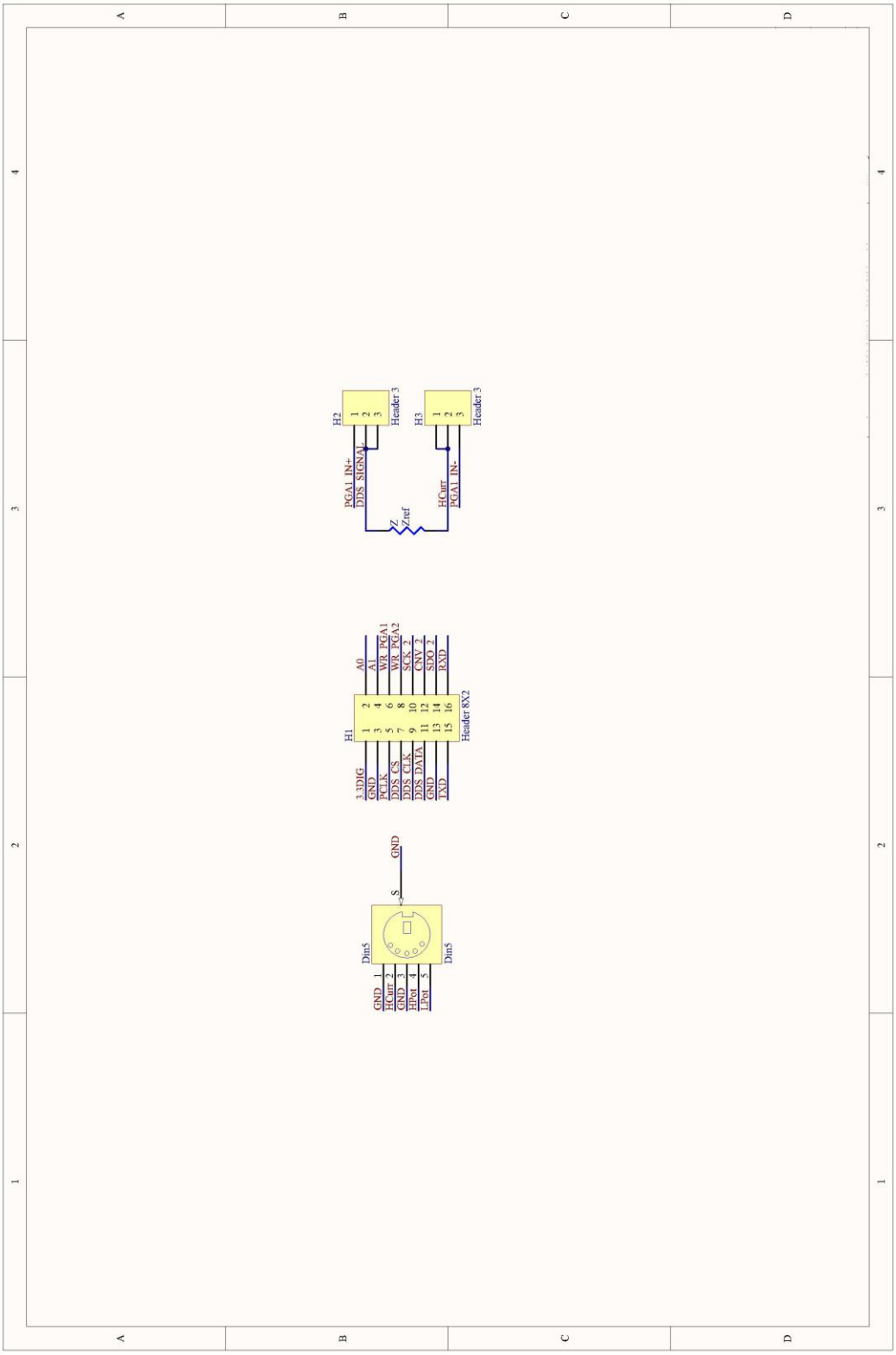

Figure 9.2 - Din5 connector, DSP connections and Impedance Reference.

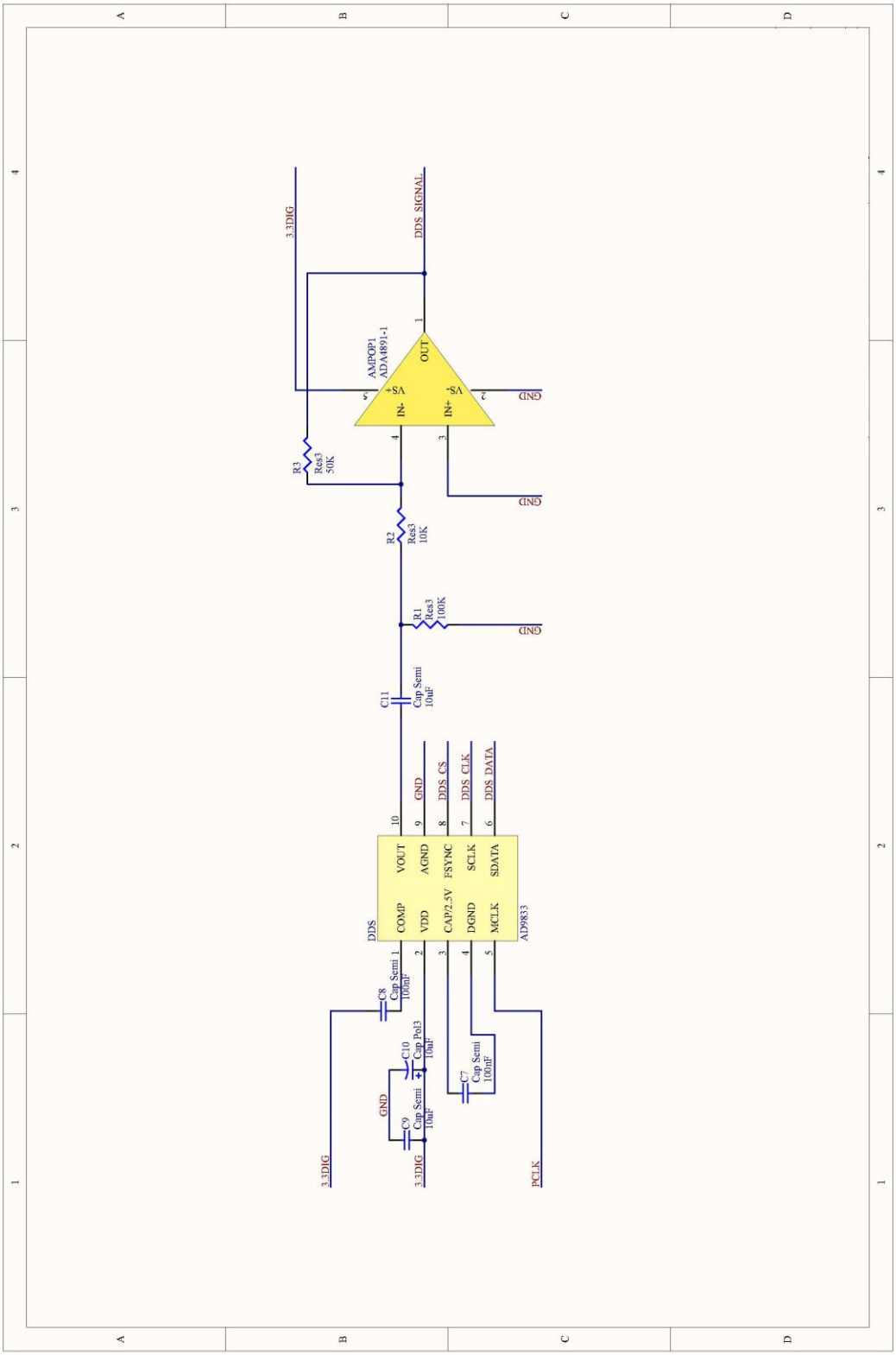

Figure 9.3 - DDS Electrical schematic.

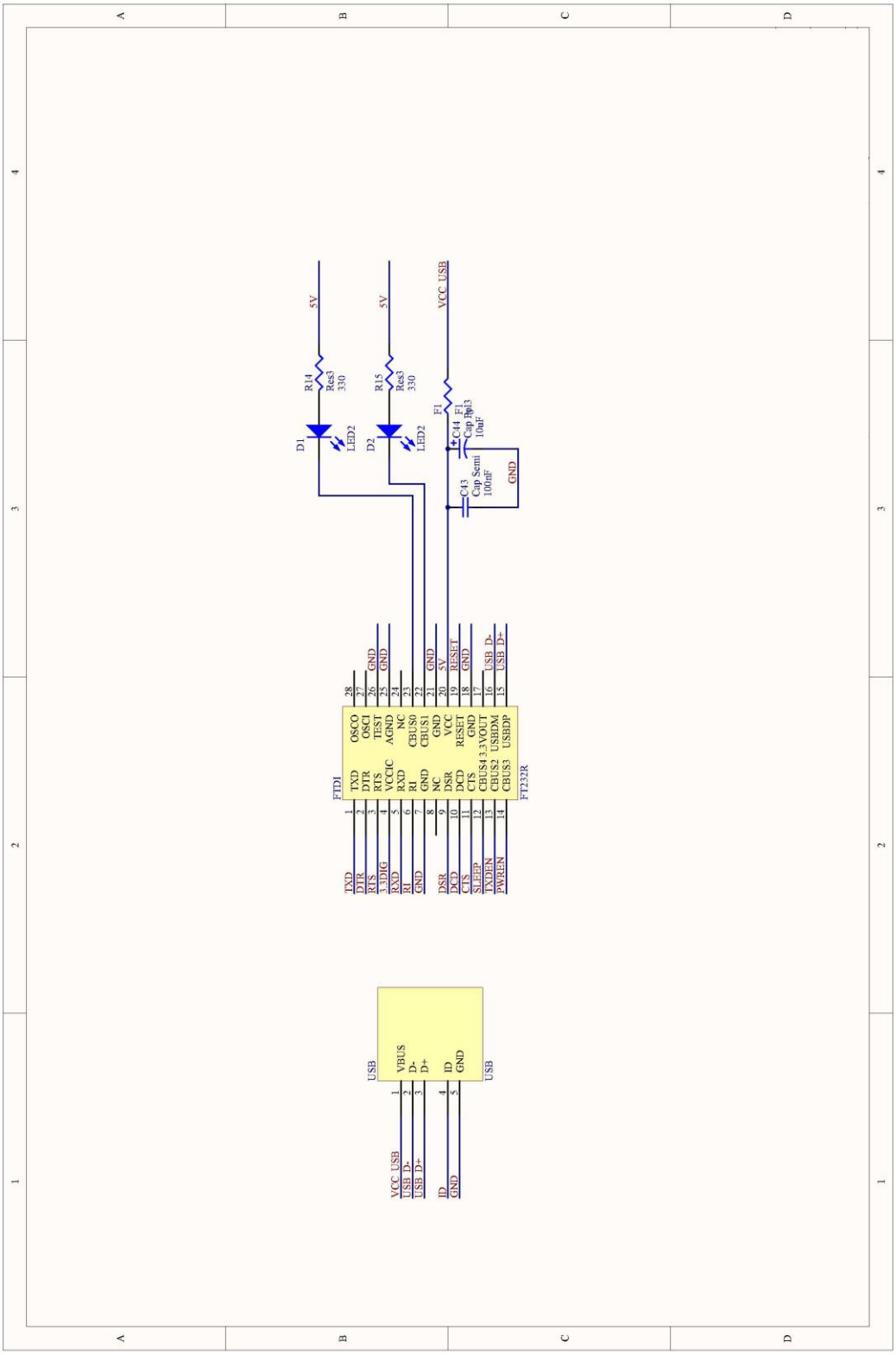

Figure 9.4 - FTDI Electrical Schematic.

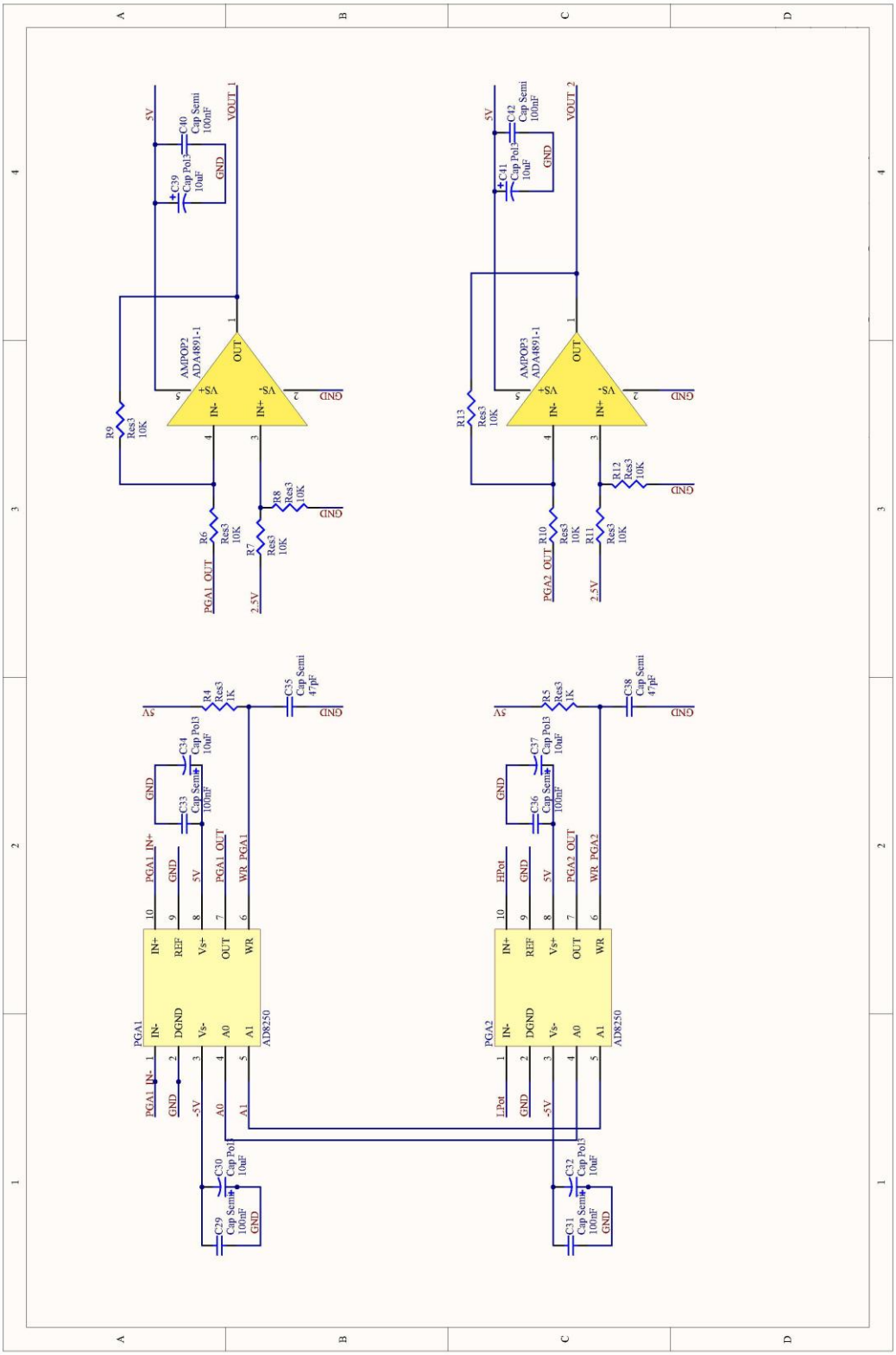

Figure 9.5 - Signal Conditioning.